Article:
Katsigiannis, G, Ferreira, P and Fuentes, R orcid.org/0000-0001-8617-7381 (2018) HYD Verifications Using Numerical Methods. Georisk, 12 (1). pp. 45-59. ISSN 1749-9526

https://doi.org/10.1080/17499518.2016.1269182

HYD Verifications Using Numerical Methods

Georgios Katsigiannis

Civil, Environmental and Geomatic Engineering Department, University College London, London, United Kingdom

georgios.katsigiannis.12@ucl.ac.uk

00447543621448

Pedro Ferreira

Civil, Environmental and Geomatic Engineering Department, University College London, London, United Kingdom

p.ferreira@ucl.ac.uk

Raul Fuentes

School of Civil Engineering, University of Leeds, Leeds, United Kingdom

r.fuentes@leeds.ac.uk

HYD Verifications Using Numerical Methods

HYD, as described in Eurocode 7, is related to the upward flow of water through the soil towards a free surface, such as in front of a retaining wall or in the base of an excavation. The HYD verification, using numerical analysis, can be performed with two different approaches. The first approach is the conventional soil block approach where safety may be checked by calculating the equilibrium of a rectangular block of soil. The second approach is the integration point approach where stability can be verified at every integration point in the numerical analysis by checking that the equilibrium is satisfied for a soil column of negligible width above each point. In this paper, the two approaches are described and their advantages and disadvantages are discussed. Comparisons made using benchmark geometries, extensively studied and discussed between the members of the EC7 Evolution Group 9, on Water Pressures, illustrate that the HYD verification using numerical methods seems very promising. Thorough comparisons between the factors from the two approaches, allow designers to better understand the benefits of using more advanced and robust approaches for such stability verifications.

Keywords: HYD; hydraulic heave; Eurocode 7; water pressures

Introduction

The HYD limit state is described in Eurocode 7 (EC7) in relation to the hydraulic heave, internal erosion and piping in the ground, caused by hydraulic gradients (BS EN 1997-1, 2004). This covers a wide range of situations related to stability problems caused by hydraulic gradients. McNamee (1949) made a distinction between two types of failure relating to water pressures; piping that usually initiates locally and heave which involves a greater soil mass.

This paper focuses on part of the EC7 definition, hydraulic heave, which is illustrated in EC7 and shown here as Figure 1. Hydraulic heave relates to the ground movement of a free surface caused by a vertical upward flow of water. Requirements for hydraulic heave are expressed in EC7 which states that the stability of a soil against

heave shall be checked in terms of seepage forces and buoyant weights, or in terms of total stresses and pore-water pressures. A particular case where hydraulic heave is relevant is in front of a retaining wall. It represents an Ultimate Limit State, potentially resulting in sudden failure with serious consequences for people and structures. Simpson et al. (1987) discussed problems caused by water pressures due to rising water levels while Stroud (1987) referred to a number of situations where unforeseen water pressures led to critical failures. Other authors have also discussed similar issues related to safety considerations in relation to the ground water pressures (e.g. Orr 2005; Simpson et al. 2009; Simpson 2011).

In recent years, with the advances in software and hardware, more designers are willing to use Finite Element (FE) methods, to verify safety against hydraulic heave. The HYD verification using FEM can be performed with two different approaches, namely the soil block approach and the integration point approach (Evolution Group 9 - Water Pressures, 2014).

The first approach is the conventional approach where safety may be checked by studying the equilibrium of a rectangular block of soil. In the integration point approach, stability can be verified at every integration point by checking the equilibrium of a soil column of negligible width. The results are plotted as contours, rendering the checks of whether the equilibrium is fulfilled at every integration point an easy task. In this chapter, the two approaches are described and their advantages and disadvantages are discussed.

Eurocode 7 requirements

Safety against failure by hydraulic heave can be verified with Equations 1 or 2 as given by EC7 (BS EN 1997-1, 2004), where stability shall be checked in terms of seepage forces and buoyant weights or in terms of total stresses and pore-water pressures.

Equation 1 (2.9a as referred to in BS EN1997-1, 2004) requires the design pore water pressure, $u_{dst;d}$ at the bottom of a relevant soil column to be less than the design total vertical stress, $\sigma_{stb;d}$. Equation 2 (2.9b as referred to in BS EN1997-1, 2004) requires the design seepage force caused by the excess pore water pressures, $S_{dst;d}$ to be less than the design buoyant weight of the column, $G'_{stb;d}$.

$$u_{dst;d} \leq \sigma_{stb;d} \quad (1)$$

$$S_{dst;d} \leq G'_{stb;d} \quad (2)$$

Both equations already incorporate safety using design values (subscript d), without further factors being shown in the requirements. The subscripts dst and stb refer to destabilising and stabilising effects respectively.

For the HYD Limit State, the typical partial factors are specified with $\gamma_{G;dst}$ =1.35 for permanent unfavourable actions, $\gamma_{G;stb}$ =0.9 for permanent favourable actions and $\gamma_{Q;dst}$ =1.5 for variable unfavourable actions (see Table 1). However, EC7 does not state precisely how these factors are to be applied in Equations 1 or 2.

Some designers apply the partial factors to the characteristic values of the stabilising and destabilising parameters, misinterpreting the Equations 1 and 2 to mean:

$$\gamma_{G;dst}\, u_{dst;k} \leq \gamma_{G;stb}\, \sigma_{stb;k} \quad (3)$$

$$\gamma_{G;dst}\, S_{dst;k} \leq \gamma_{G;stb}\, G'_{stb;k} \quad (4)$$

Here, the subscript k refers to characteristic values of the parameters. Orr (2005) pointed out that if the two equations are used in this way they can lead to markedly different results for the same values of partial factors. Simpson (2012) argues that this is a misunderstanding of the code requirement, and in particular of the concept of design values, and suggested that if the load partial factors are to be used in this context, they

should be applied to the excess water pressures only, not to the hydrostatic component. Orr (2005) also concluded that the partial actions factors should only be applied to the excess pore water pressure and not the hydrostatic pressure.

EC7 notes that the load factors might not be always appropriate for ground water pressures and allows for direct assessment of the design value or application of a safety margin to the characteristic ground water table. Thus, by allowing three alternative approaches, the UK National Annex leaves much of the responsibility for calculation of the design value of water pressures with the designers (Simpson et al. 2011). Simpson and Katsigiannis (2015) argue that factoring water pressures should generally be avoided and favour the direct assessment of the design water pressures or the design water table level.

Methodology

The two approaches for HYD verification using FE methods, are now illustrated for the two simple problems presented in Figure 2, a 10m excavation and a cofferdam geometry. The software used is Plaxis 2015.02 and the following assumptions were made in the model:

- The wall is wished-in-place, impermeable and not allowed to deform in any direction.
- Only half of the excavation width is modelled due to symmetry.
- The calculations are performed assuming steady state conditions while the soil is considered fully drained; constant hydraulic head is used by specifying a fixed water table level behind the retaining wall. In front of the wall, the water level is defined in the formation level, at the end of the excavation.
- The side and bottom model boundaries are considered to be impermeable.
- The side model boundaries are fixed in the x direction while the bottom model boundary is fixed in both x and y directions.
- The unit weight of the soil γ is equal to 20kN/m^3

- Initial stress field conditions are based on hydrostatic water pressures and K_0=1-sinφ'.
- Interface elements are used between the soil and the wall with tanδ = 0.5tanφ', where δ is the soil/wall friction angle.

The properties of the soil are given in Table 2 for an elastic-perfectly plastic soil model such as the Mohr-Coulomb. The stiffness of the soil, which varies with depth, has no effect on this problem. The Finite Element mesh used for the simulations, which consists of 4332 15-node triangular elements, is given in Figure 3 for the 10m deep excavation case. The current mesh size is adequate for this type of problem.

The Soil Block Approach

The Terzaghi's criterion

According to experimental evidence for isotropic and uniform soils, it is sufficient to check the stability of a rectangular soil block of dimensions b=t/2, where b is the block's width and t the embedment depth (Terzaghi 1922, 1943), by ensuring that the buoyant weight of the block is greater than the seepage force (see Figure 4). The friction on both sides of the block is not taken into account. Terzaghi proposed that a factor of safety should be calculated as $F_T = G'/S$, where G' is the buoyant weight of the block and S is the upwards seepage force. Other authors also presented results from tests on homogeneous sands. Marsland (1953) also observed that the soil fails as a block while Davidenkoff (1954) highlighted that the shear forces on the sides of the block should be ignored.

Although Terzaghi et al. (1996), gives a worked example in which the acceptable factor required is F_T=2.5, no direct recommendation from Terzaghi has been found, in previous publications, with the specification of a minimum factor of safety. Values taken from a survey of publications, generally based on the use of Terzaghi's

diagram, are summarised in Table 3 (Simpson and Katsigiannis, 2015). The values for the required factor of safety shown in Table 3, range from 1.42 to 5. While some authorities require larger factors for finer soils than for coarser soils, no explanation of this range has been given by the above mentioned authors.

Skempton and Brogan (1994) illustrated the significance of the grading curves of the materials in relation to safety considerations in the presence of hydraulic gradients. Even if water pressures are known with confidence, the achieved levels of safety highly depend on the grading curve of the material, with poorly graded materials generally tolerating lower hydraulic gradients. This is because, in poorly graded materials, the effective stress may vary locally over distances of the order of a few soil particles, leaving some particles at much lower stresses than normally calculated from the depth of overburden.

Similarly, the German guide on erosion (BAW, 2013) makes a distinction between poorly graded soils that are internally unstable and well graded soils where the soil particle mixtures are internally stable. The critical failure mechanism depends on the grading curve with internal erosion and particularly suffusion (migration of fines due to seepage forces through the pores of a coarse particles structure) being critical for poorly graded soils and hydraulic heave for well graded soils.

This variability of the grading curves and the governing failure mechanisms among different soils, may explain why different authors have proposed quite different values for the Terzaghi's factor with higher values typically suggested as an empirical way to account for the anomalies in grading curve or internally unstable soils.

The Soil Block approach with FEM

The Soil Block approach is based on the conventional Terzaghi's approach where safety may be checked by studying the equilibrium of a rectangular block of soil. In the soil

block approach, the Terzaghi's factor (F_T) at steady state directly relates to the $\gamma_{dst}/\gamma_{stb}$ ratio where γ_{dst} is the partial factor applied to the destabilising seepage force and γ_{stb} the partial factor applied to the stabilising buoyant weight of the block. Expressing the partial factors as a ratio enables comparisons with the global safety factor values traditionally used for similar problems in a number of countries and for a range of different materials.

Calculating the Terzaghi's factor (F_T) with FE methods is straightforward. The definition of the factor is given in Equation 5, where W is the weight of the soil block, H is the force on the base of the block due to hydrostatic pressure, U is the water force on the base of the block, W-H is the buoyant weight and U-H is the seepage force.

$$F_T = \frac{W-H}{U-H} \tag{5}$$

The weight of the soil block W and the hydrostatic force on the base of the block H, and hence the buoyant weight of the block W-H, can be easily calculated as the unit weight of the soil and the water are known. The water force on the soil block U is obtained from the output of the FE analysis.

As mentioned before, Terzaghi recommended that a column of width b=t/2 should be used in the calculations of the factor of safety, taking no account of friction forces on its vertical sides. It could be that Terzaghi considered that a narrower column is unlikely to fail given that the friction forces acting on the sides of the block would become significant. The reason for this, however, is unclear, therefore for this study, all the soil block calculations are based on the Terzaghi's block dimensions, where the depth of the block is equal to the embedment depth t and the width b is equal to t/2.

As the buoyant weight, which is a stabilising force, only depends on the unit weight of the soil, γ, and can be easily calculated for the Terzaghi's block as defined in Figure 4. The Terzaghi's factor is more sensitive to variations of the destabilising force which is the seepage force caused by the pore water pressures. The effects of different parameters on the pore water pressures and hence the Terzaghi's factor, are investigated in this study.

Effect of Δh/t

In this section, the effect of varying the ratio Δh/t on the calculated Terzaghi's factor is investigated for the 10m excavation and cofferdam reference geometries (see Figure 2). In the cofferdam case, there is no excavation of the soil so that the ground surface is at the same level on both sides of the wall and the water flows around the wall because of the difference in the hydraulic head.

By gradually increasing the Δh/t ratio, both analyses were driven to failure. Different hydraulic heads were used by specifying different water table levels behind the retaining wall. At the end of each analysis, the Terzaghi's factor was calculated by integrating the pore water pressures acting along the base of the soil block, from the output of the calculations.

In Figure 5, the calculated Terzaghi's factor is plotted against the ratio Δh/t. It can be seen that, in both cases, the factor decreases with increasing Δh/t with the factor values being consistently higher for the 10m deep excavation case. Moreover, the cofferdam and excavation problems become unstable, i.e. F_T=1, for a ratio of Δh/t equal to 2.25 and Δh/t=3.3 respectively. In both cases, the pore pressures become high, reducing the effective stresses, and making the values of wall friction insignificant.

Simpson and Katsigiannis (2015), considering a 10m deep excavation, wide enough to give only minor lateral restraint to the flow (x = 4t), observed that the factor

of safety becomes, as expected, lower as the difference in the hydraulic head becomes higher. It was observed that the FE analysis becomes unstable for a Δh/t ratio in excess of 3.3 which is consistent with this study.

Effect of minimum flow path

The reason that in Figure 5, the 10m deep excavation case gives higher values of the Terzaghi's factor than the cofferdam case for the same ratios of Δh/t, is that the minimum flow paths are different. The minimum flow path which can be defined as the shortest subsurface path a water particle would follow, in a given groundwater regime, is equal to the sum of the distance from the tip of the wall to the groundwater table level in front of the wall, and the distance from the tip of the wall to the groundwater table level behind the wall. This means that for a given ratio of Δh/t, the minimum flow path relates directly to the height of the retained soil behind of the wall.

In Figure 2, the minimum flow paths are illustrated with the light solid lines around the wall for the 10m excavation and the cofferdam problem respectively. For example, for Δh/t=1.5, the minimum flow path is 6m for the cofferdam case and 10.5m for the 10m deep excavation case. Longer flow paths for the same Δh/t, indicate higher loss of energy through the voids formed by the soil particles and hence relief in the pore water pressures acting at the bottom of the soil block.

To better illustrate this effect, the analyses were repeated for variations in the minimum flow paths, achieved by increasing gradually the height of the soil retained behind the retaining wall. The calculated values of Terzaghi's factor are plotted in Figure 6 against the minimum flow path for the different ratios of Δh/t. It can be seen that the minimum flow path is 6m for the cofferdam case, regardless of the level of the water behind the wall, while for the 10m deep excavation, the minimum flow path was measured as 9, 10.5 and 12 for ratios of Δh/t equal to 1, 1.5 and 2 respectively.

Moreover, for the same Δh/t, the Terzaghi's factor becomes lower as the minimum flow path decreases with the cofferdam case being the most critical.

Effect of excavation width

In this section, the effect of varying the excavation width on the calculated Terzaghi's factor is investigated for the two reference geometries in Figure 2.

Figure 7 shows head equipotential lines for three cases: (a) a wide excavation (width x=12t), (b) a narrow trench (x=t), and (c) a circular excavation (diameter d=t). In all cases, the seepage is generated from a side boundary located at 18m (6t) from the wall, where a constant head is applied. For Δh=1.5t, the Terzaghi's factor of safety F_T is: (a) 2.89; (b) 1.33 and (c) 0.97, respectively (Simpson and Katsigiannis 2015).

Similarly, Aulbach and Ziegler (2013) found that when water is flowing upwards, beneath a narrow excavation, the upward hydraulic gradients are higher than in the cases of wider excavations with little or no lateral restraint.

To better illustrate this effect, the analysis is repeated for different x/t ratios where x is the excavation width in the horizontal direction (only half the excavation is modelled due to symmetry) and t is the embedment depth in the vertical direction while the rest of the model parameters remain the same. More specifically, 5 different cases were considered for plain strain conditions: x/t=12, 8, 4, 2 and 1. At the end of each analysis, the Terzaghi's factor was calculated using the values of the pore water pressures acting at the bottom of the soil block from the output of the calculations. This study includes 10 different geometries each simulated using three different values of Δh/t, totalling 30 analyses.

In Figure 8, the Terzaghi's factor is plotted against the ratio x/t for Δh/t=1.5. It can be seen that, the narrower the excavation is, the lower the factor of safety becomes. The values of factor of safety show larger drops for values of x/t lower than 4 on both

geometries. Figure 9 presents the values of the Terzaghi's factor for different values of x/t and Δh/t for the excavation case. Again, it can be seen that the factor of safety drops significantly as the excavation becomes narrower.

Discussion

It can be concluded that the use of the Soil Block approach with FE methods is straightforward, requiring only the pore water pressure from the numerical analysis for the calculation of the Terzaghi's factor of safety. The calculated Terzaghi's factor directly depends on the upstream and downstream groundwater levels as specified by the ratio Δh/t. It was also noted that for a given difference in the hydraulic head, the system becomes more critical for shorter minimum flow paths and narrow excavations, where confined spaces result in an increase in the groundwater pressures.

The obvious disadvantage of the Soil Block Approach is that it provides no useful information about the critical failure mechanism and it is only applicable to very specific situations of upward flow towards a horizontal surface. In practice, more complex situations are encountered, including flow beneath sloping surfaces in embankments and cuttings.

The Integration Point Approach

The second approach for verifying stability against HYD using FEM, is the integration point approach which can be expressed in two different forms, depending on how safety is introduced into the calculations. According to EC7, design ground-water pressures may be derived either by applying partial factors to characteristic water pressures or by applying a safety margin to the characteristic water level (BS EN1997-1 2.4.6.1(8)).

In the first form of the Integration Point Approach, safety is verified at every integration point for a given set of partial load factors applied to the destabilising and stabilising actions. Hence, the design water pressures are calculated after applying the corresponding factor to their characteristic values, derived from the output of the FE calculations.

In the second form, no factors are applied to the water pressures but their design values are derived by directly assessing the design water table which is input in the numerical calculations. Thus, the values derived from the output of the FE analysis are already design values and no further factors need to be applied. Afterwards, the stabilising and destabilising pressures are combined at every integration point to give the achieved factor of safety as an estimate of the level of safety and economy.

In both cases, as outputs of the numerical analysis are used for the safety verification, care must be taken when selecting the appropriate boundary conditions and mesh coarseness as these will affect the calculated values.

Apply partial factors to the excess pore water pressures

In the first form of the approach, stability is verified at every integration point by checking that a relevant criterion with a given combination of partial factors, is fulfilled for a soil column of negligible width above each point. Then contours of the criterion values can be plotted downstream, in front of the wall, to check whether the criterion is fulfilled.

Simpson (2012) shows that when water pressures have to be factored, γ_{dst} should be applied to the excess pore water pressure because the destabilizing seepage force is only caused due to the excess pore water and not the hydrostatic component of the water pressure. Similarly, the stabilising factor, γ_{stb} should be applied to the buoyant density of the soil γ'. Based on the above, this study only focuses on the comparison of the two

criteria, namely the D_γ and D_σ, defined in Equations 6 and 7 respectively. The values of the partial factors γ_{stb} and γ_{dst}, used in both Equations, correspond to the values required by EC7 and are given in Table 2.

$$D_\gamma = \gamma_{stb}(\gamma z - \gamma_w z) - \gamma_{dst}(u_k - \gamma_w z) > 0 \quad (6)$$

$$D_\sigma = \gamma_{stb}(\sigma_v - \gamma_w z) - \gamma_{dst}(u_k - \gamma_w z) > 0 \quad (7)$$

The difference between the two criteria is that in D_γ, the total vertical stress, σ_v is equal to γz, while in D_σ the σ_v value is taken from the output of the numerical analysis (i.e. it includes other elements such as friction). No evidence is presented in the literature on which criterion is more suitable. Stelzer and Odenwald (2015) used the D_σ criterion (referred to as simply D in their paper) for verifying safety against HYD for a cofferdam geometry as a way to take into consideration the stress redistribution and the friction. However, a thorough comparison of the two criteria is needed to better understand their advantages and limitations.

In Figures 10 to 13, the contours of the D_γ and D_σ criteria are presented for the two extreme cases considered in section 4: the 10m deep excavation and the cofferdam case with x/t=4. For illustration purposes, only the contours for the cases that correspond to a Terzaghi's factor equal to 1.5 are presented here. It can be seen in Figure 6, that the Terzaghi's factor becomes 1.5 for Δh/t=1.8 and Δh/t=1.5 for the 10m excavation and the cofferdam case respectively. This is because the minimum flow path is shorter for the cofferdam geometry and hence the hydraulic heave problem becomes more critical.

Note that the contours are only plotted for the area of interest in front of the wall, where the vertical dimension of the area in the y axis direction, is twice the embedment depth and the horizontal dimension in the x axis direction is half the excavation width.

It can be seen from Figure 10 and Figure 11 that while both cases correspond to a value of Terzaghi's factor equal to 1.5, when the contours of D_γ are plotted using the partial factors required by EC7 (where $\gamma_{dst}/\gamma_{stb}$=1.5), there is an area close to the wall where the safety criterion is not fulfilled (zone with negative values).

In Figures 12 and 13, the contours of D_σ are plotted using again the EC7 partial factors and the effect of using the σ_v values from the output of the FE analysis instead of γz, is illustrated. For the 10m excavation case, it can be seen from Figure 12 that the contours of D_σ are everywhere positive and the criterion everywhere fulfilled. This means that using σ_v instead of γz to calculate the stabilizing stresses has a significantly favourable effect. On the other hand, for the cofferdam case, when the contours of D_σ are plotted (Figure 13), it is observed that while the negative area is smaller compared to the contours of D_γ in Figure 11, the criterion is still not fulfilled everywhere. It is obvious that while γz is uniquely defined, σ_v varies and can have a favourable effect when being used instead of γz.

Please note that negative values of either D_γ or D_σ relate to a local failure at the specific integration point and not to the global failure of the soil in the area in front of the wall. That is why an essential part of the HYD verification using the Integration Point approach is the contour plotting of the criteria values.

Direct assessment of the design water table

EG9 of EC7, in its final report, has proposed that no factors should be applied to water

pressures (Evolution Group 9 - Water Pressures, 2014). The members of EG9 have recommended that in situations of this type, partial safety factors should not be applied to water pressures or to forces derived from water pressures, such as the seepage force S. Instead, engineers must take an appropriately cautious view of the piezometric water table level and the water pressures that could occur in the ground. According to EG9, the characteristic piezometric water levels and accordingly the characteristic values of water pressures shall correspond to a return period at least equal to the duration of the design life span of the structure (e.g. 100 years) while the ultimate limit state piezometric water levels and accordingly the ultimate limit state values of water pressures shall have a rare probability (e.g. 1%) of occurrence in the duration of the design situation of the structure. This also implies that a careful review of the possible range of distributions of permeability must be undertaken (e.g. even thin layers of lower permeability can cause the generation of high water pressures) and the design must be based on the worst that is credible. Afterwards, the code requirement is simply to prove that equilibrium exists under those design conditions.

An alternative form of the integration point approach, described previously, can be used in combination with such directly specified design water table, to give an estimate of the achieved level of safety at every integration point of the FE mesh in the area in front of the wall. Based on the definitions of D_γ and D_σ (Equations 6 and 7), the integration point approach factors of safety, namely $F_{D\gamma}$and $F_{D\sigma}$ are defined in Equations 8 and 9.

$$F_{D\gamma} = \frac{\gamma z - \gamma_w z}{u_k - \gamma_w z} \tag{8}$$

$$F_{D\sigma} = \frac{\sigma_v - \gamma_w z}{u_k - \gamma_w z} \tag{9}$$

According to these definitions, $F_{D\gamma}$ and $F_{D\sigma}$ are equal to the ratio $\gamma_{dst}/\gamma_{stb}$ when the criteria D_γ and D_σ respectively, are equal to zero. Hence, the contours of $F_{D\gamma}$ and $F_{D\sigma}$, provide the safety factor value achieved at each integration point. Again, the two Equations differ in the way they include the total vertical stress in the calculations. Equation 8 ignores the mobilised friction effects whilst Equation 9 introduces σ_v directly from the output of the FE analysis, hence accounting for the friction developed along the soil/wall interface.

In Figures 14 and 15, the contours of $F_{D\gamma}$ are plotted for the 10m deep excavation and the cofferdam case for a ratio of Δh/t equal to 1.8 and 1.5 respectively. It can be seen that, in both cases, a minimum value of $F_{D\gamma}$ equal approximately to 1.3 is achieved. The lowest value of the factor of safety is close to the toe of the wall where the excess pore water pressures have their highest values.

Similarly, in Figures 16 and 17, the contours of $F_{D\sigma}$ are plotted for the same cases. However, the calculated values of the safety factor are now different for the two problems. For the 10m excavation case, the minimum factor is 1.8 (see Figure 16) while for the cofferdam case it is 1.4 (see Figure 17). Both values are higher than the corresponding minimum $F_{D\gamma}$ value observed in Figure 14 and 15 for the same Δh/t. However, $F_{D\sigma}$ is much higher for the 10m excavation than the cofferdam case because of the favourable effect of the mobilised friction.

Comparison of the factors

It was observed above that for cases corresponding to a Terzaghi's factor of 1.5, there is an area close to the wall where $F_{D\gamma}$is less than 1.5, while when calculating the $F_{D\sigma}$ values, it was observed that the factor varies depending on the effect of the mobilised friction. It is clear that there is a need for a more thorough comparison

between the calculated values of the safety factors from the Soil Block and the Integration Point approaches, together with a better understanding of the resulting differences.

In this section, the minimum integration point factors $F_{D\gamma}$ and $F_{D\sigma}$ (i.e. close to the toe of the wall) are plotted against the Terzaghi's factor F_T for the 10m excavation and cofferdam cases with varying x/t, Δh/t and the soil/wall interface friction angle δ. In Figure 18, the relationship between $F_{D\gamma}$ and F_T is presented. As can be seen, the points follow a linear trend, where $F_T = 1.15F_{D\gamma}$, with an R^2 value of 0.98. Since friction is not considered, only one line defines the relationship between the two factors. According to their definition, both factors are calculated using γz as the stabilizing stress. However, as the factor $F_{D\gamma}$ is calculated at every integration point of the FE mesh, instead of a soil block, a value of 1.0 is only related to a very local failure at the specific integration point and not the global failure of the soil in the area in front of the wall.

In Figure 19, the relationships are given between the Terzaghi's factor F_T and the integration point approach factor, $F_{D\sigma}$ for both geometries. Straight lines are a good approximation (with R^2 values between 0.89 and 0.98). However, due to the presence of friction, the relation is not unique. $F_{D\sigma}$ is higher for the 10m excavation case than the cofferdam case as the friction effect is more significant. When tanδ increases from 0.5tanφ' to tanφ', both lines move to the right as $F_{D\sigma}$ values increase (dashed lines).

The reason for this is that the effective horizontal stresses acting on the wall, and therefore, the mobilised friction, are different. While the earth coefficient at rest is the same and equal to 1-sinφ', the initial effective horizontal stresses are different as they are calculated at different depths. Since the initial stresses are calculated before the excavation is made, the toe of the wall is 13m and 3m below the ground level for the 10m deep excavation and the cofferdam case respectively. After the excavation of 10m

of soil, the horizontal effective stresses are 'locked-in'. They don't completely disappear when the loading is removed.

To illustrate this effect, Figure 20 presents the effective horizontal stress profiles in front of the wall and the resultant forces for all cases. It can be noted, that the effective horizontal stresses are much higher for the 10m excavation than the cofferdam case. Moreover, when tanδ increases from 0.5tanφ' to tanφ', the total force increases from 13.1kN/m to 21.8kN/m in the case of the cofferdam and from 69.4kN/m to 137.5kN/m in the case of the 10m deep excavation. This increase in horizontal stresses is directly proportional to the friction between soil and wall. The findings agree with the results of Benmebarek et al. (2005) who carried out parametric analysis to investigate the effect of wall friction for a similar problem and Stelzer and Odenwald (2015) who observed a higher effect of friction in a supported excavation, when compared to a cofferdam geometry, resulting in higher stresses in the proximity of the wall.

The analysis was also repeated for a weaker soil to investigate the effect of the soil strength parameters on the calculated values of $F_{D\gamma}$ and $F_{D\sigma}$ and the relationship with F_T. The new soil has an angle of shearing resistance equal to φ'=25° while the rest of the soil parameters, listed in Table 2, remain the same. The analysis is repeated for both the 10m excavation and the cofferdam case with varying Δh/t, x/t and δ.

Since $F_{D\gamma}$ is not related to the friction angle but to the unit weight of the soil, the relationship determined in Figure 18 can be used for this soil. However, as illustrated in Figure 21, the effect is significant for $F_{D\sigma}$. It can be seen that the solid $F_{D\sigma}$ lines for the 10m excavation and the cofferdam case, have moved to the left of the graph and hence the $F_{D\sigma}$ values have decreased when compared to Figure 19. The decrease in the angle of shearing resistance and hence the decrease in soil/wall friction angle, reduces the calculated factor of safety $F_{D\sigma}$ and therefore has an unfavourable

effect on the calculated $F_{D\sigma}$ values. It is worth noting that when tanδ increases from 0.5tanφ' to tanφ', both $F_{D\sigma}$ lines move to the right as $F_{D\sigma}$ values increase (dashed lines). The effect is again particularly significant for the 10m excavation case where σ_v is much higher than γz due to the friction component. It is important to mention that all the other geometries considered, for the minimum flow path parametric analysis, yielded values that fell between the $F_{D\sigma}$ lines in Figures 19 and 21.

In all cases considered, for the same F_T value, the calculated values of $F_{D\sigma}$ are higher than the corresponding values of $F_{D\gamma}$, meaning, in principle, that $\sigma_v > \gamma z$. As the effect of friction becomes more significant, either by increased effective horizontal stresses or soil/wall interface friction angle δ, σ_v becomes much higher than γz and hence $F_{D\sigma}$ is much higher than $F_{D\gamma}$.

However, it is interesting that the range of $F_{D\sigma}$ values, from all cases considered, narrows down for lower values of F_T (especially lower than 1.5) and also their values become closer to the corresponding $F_{D\gamma}$ values. In fact, they almost have a common point at $F_{D\sigma} = F_{D\gamma} = 1$, $F_T = 1.15$. At this point, friction against the wall is destroyed by water pressure.

Discussion

The results show that there is a unique and simple relationship between F_T and $F_{D\gamma}$, proportional to the unit weight of the soil. With regards to $F_{D\sigma}$, the calculations using two extreme geometries, two different angles of shearing resistance φ' and soil/wall interface friction angles δ, have shown that the range of relationships between the factors is broad and very sensitive to effect of friction along the wall.

Moreover, the $F_{D\gamma}$ values are lower than those of $F_{D\sigma}$ for all cases considered and hence they provide a conservative verification of the HYD Limit State. However,

when pore water pressures rise, the effective stresses decrease and the friction effect is lost. In this instance, the HYD Limit State becomes more critical and all the $F_{D\sigma}$ lines tend to converge towards the $F_{D\gamma}$ line.

The use of the $F_{D\gamma}$ factor of safety presents advantages over the use of the $F_{D\sigma}$ factor as, in general, designers should not just rely on the favourable friction effect to verify stability against HYD. Remote from the limit state, wall friction appears to enhance safety, increasing $F_{D\sigma}$. But at the limit state, this is no longer so because the water pressure destroys the friction. This illustrates the fact that carrying out calculations for conditions remote from the limit state and then relying on a factor of safety can be misleading.

Concluding remarks

The verification of stability against HYD using FE methods is straightforward and seems very promising. While designers might be more familiar with the Soil Block approach and the Terzaghi's calculation, the more advanced Integration Point approach has the advantage that it is readily applicable not only to the simple cases considered here, but also to more complicated situations such as water approaching sloping ground surfaces. Moreover, it provides insights about the stability of the soil at a very local level, instead of assuming a pre-defined failure mechanism (e.g. a block of soil mass with specific dimensions).

There are two ways to introduce design values of the destabilising pore water pressures into the Integration Point approach calculations; either by applying the HYD partial load factors suggested by EC7 to the characteristic values or by directly assessing the design water table. As it is very likely, based on the suggestions of the EG9 (Evolution Group 9 - Water Pressures, 2014), that the next version of the Eurocode

7, due in 2020, will move away from factoring the pore water pressures, the calculation of the integration point factors, based on a direct assessment of the groundwater conditions, might become more relevant in the future compared to the verification using the D_γ and D_σ criteria, which involve the application of partial factors. Moreover, the integration point approach criteria and factors of safety are calculated based on the excess pore water pressures. Therefore, the Integration Point approach addresses the misinterpretation mentioned above regarding which component of the pore water pressure needs to be factored.

The use of the $F_{D\gamma}$ safety factor to get an estimate of the safety margin has significant advantages, in the opinion of the authors, since there is no friction available at the limit state.

Further research

This paper presents a comprehensive study on the subject focusing on plain strain two dimensional problems. Further studies need to address the applicability of the conclusions for axi-symmetry problems (e.g. circular excavations). Moreover, Aulbach and Ziegler (2014) have investigated that hydraulic heave is most critical in the corners of excavation pits. Therefore, a further study should also examine whether the conclusions are also applicable for 3D problems.

Acknowledgements

The authors gratefully acknowledge the support of the project partners, EPSRC and Arup. Special thanks are extended to Brian Simpson from Arup Geotechnics and the other members of the EC7 Evolution Group 9 for the useful discussions.

References

Aulbach, B., and Ziegler, M. 2013. Simplified design of excavation support and shafts for safety against hydraulic heave. Geotechnics and Tunnelling, 362-374.

Aulbach, B., Ziegler, M. 2014. Versagensform und Nachweisform beim hydraulischen Grundbruch – Plädoyer für den Terzaghi-Körper, Geotechnik, 6-18.

BAW. 2013. Code of Practice: Internal Erosion (MMB). German Federal Waterways Engineering and Research Institute, Karlsruhe

Benmebarek, N., Benmebarek, S., and Kastner, R. 2005. Numerical studies of seepage failure of sand within a cofferdam. Computers and Geotechnics, 264-273.

BS EN1997-1, Eurocode 7 – Geotechnical design, Part 1 – general rules. 2004. London: British Standards Institution.

Das, B. 1983. Advanced Soil Mechanics. McGraw-Hill.

Davidenkoff, R.N. 1954. Zur berechnung des hydraulischen grundbruches. Wasserwirtschaft 1954(46):298–307.

Evolution Group 9 - Water Pressures. 2014. Final report to TC250/SC7 Evolution of Eurocode 7 Part 1. July 2014.

Harr, M. 1962. Groundwater and Seepage. McGraw-Hill.

Kashef, A. 1986. Groundwater Engineering. McGraw Hill.

Marsland, A. 1953. Model experiments to study the influence of seepage on the stability of a sheeted excavation in sand. Géotechnique. The Institution of Civil Engineers. London 1953; 4(7):223–41.

McNamee, J. 1949. Seepage into a sheeted excavation. Géotechnique. The Institution of Civil Engineers. London 1949; 4(1):229–41.

Odenwald, B., and Stelzer, O. 2013. Nachweis gegen hydraulischen Grundbruch mit FEM auf Grundlage des EC 7. Workshop Bemessen mit numerischen Methoden (pp. 88-110). Veröffentlichungen des Institutes Geotechnik und Baubetrieb TU Hamburg

Orr, T. 2005. Model Solutions for Eurocode 7 Workshop Examples. Dublin: Trinity College.

Ryner, A., Fredriksson, A., and Stille, H. 1996. *Sponthandboken: handbok för* konstruktion och utformning av sponter. Byggforskningsrådet T18:1996.

Simpson, B., Blower, T., Craig, R.N. and Wilkinson, W. B. 1989. The engineering implications of rising groundwater levels in the deep aquifer beneath London. CIRIA Special Publication 89, 1989.

Simpson, B., Morrison, P., Yasuda, S., Townsend, B., and Gazetas, G. 2009. State of the art report: Analysis and design. Proc. 17th Int. Conf. SMGE, Alexandria, Vol 4, pp. 2873-2929.

Simpson, B., Vogt, N. and Van Seters, A.J. 2011. Geotechnical Safety in Relation to Water Pressures. Proceedings of the 3rd International Symposium on Geotechnical Safety and Risk. Munich.

Simpson, B. 2011. Water pressures. Proc. 2nd International Workshop on Evaluation of Eurocode 7. Pavia. 12-14 April 2010.

Simpson, B. 2012. Eurocode 7 – fundamental issues and some implications for users. 16th Nordic Geotechnical Meeting (pp. 29-52). Copenhagen: Danish Geotechnical Society.

Simpson, B., and Katsigiannis, G. 2015. Safety Considerations for the HYD Limit State. XVI European Conference on Soil Mechanics and Geotechnical Engineering (pp. 4325-4330). Edinburgh: ICE Publishing.

Skempton, A. W., and Brogan, J. M. 1994. Experiments on piping in sandy gravels. Géotechnique. 44, No. 3,449-460.

Stelzer, O., and Odenwald, B. 2015. A New Stress-Based Approach for Verification of Safety Against Hydraulic Heave Based on EC7. XVI European Conference on Soil Mechanics and Geotechnical Engineering (pp. 4073-4078). Edinburgh: ICE Publishing.

Stroud, M.A. 1987. The Control of Groundwater. General Report and State of the Art Review to Session 2 of IX ECSMFE Dublin.

Terzaghi, K. 1922. Der Grundbruch an Stauwerken and seine Verhiltung. Die Wasserkraft, 445-449.

Terzaghi, K. 1943. Theoretical Soil Mechanics. New York: J. Wiley and Sons.

Terzaghi, K., Peck, R., and Mesri, G. 1996. Soil Mechanics in Engineering Practice, 3rd edition. John Wiley & Sons, Inc.

Williams, B., and Waite, D. 1993. The design and construction of sheet-piled cofferdams. London: Special publication 95. Construction Industry Research and Information Association.

Table 1. Partial factors for HYD

Action	Symbol	Value
Permanent		
Unfavourable[a]	$\gamma_{G;dst}$	1.35
Favourable[b]	$\gamma_{G;stb}$	0.90
Variable		
Unfavourable[a]	$\gamma_{Q;dst}$	1.50

a Destabilising b Stabilising

Table 2. Mohr-Coulomb model parameters

Soil Properties	
Young's Modulus, E' (MPa)	25+6.5z
Angle of shearing resistance, φ' (°)	35
Effective cohesion, c' (kPa)	0
Poisson's ratio, v'	0.2
Permeability (m/s)	10^{-5}

where z is the depth below the ground level (m)

Table 3. Published values for Terzaghi's factor of safety F_T (update of the table given by Simpson & Katsigiannis, 2015)

Publication and any limitations		Values
Williams & Waite (1993)		1.5 to 2.0
For clean sands		
Kashef, Abdel-Aziz Ismail (1986)		4 to 5
Harr (1962)		4 to 5
German practice	– unfavourable soils	2
(DIN 1054/A2 2015-11)	– favourable soils	1.53
Swedish practice	– coarse soils	1.5
(Ryner et al 1996)	– silty material	2.5
Dutch practice		2.8
Das (1983), quoting Harr (1962)		4 to 5

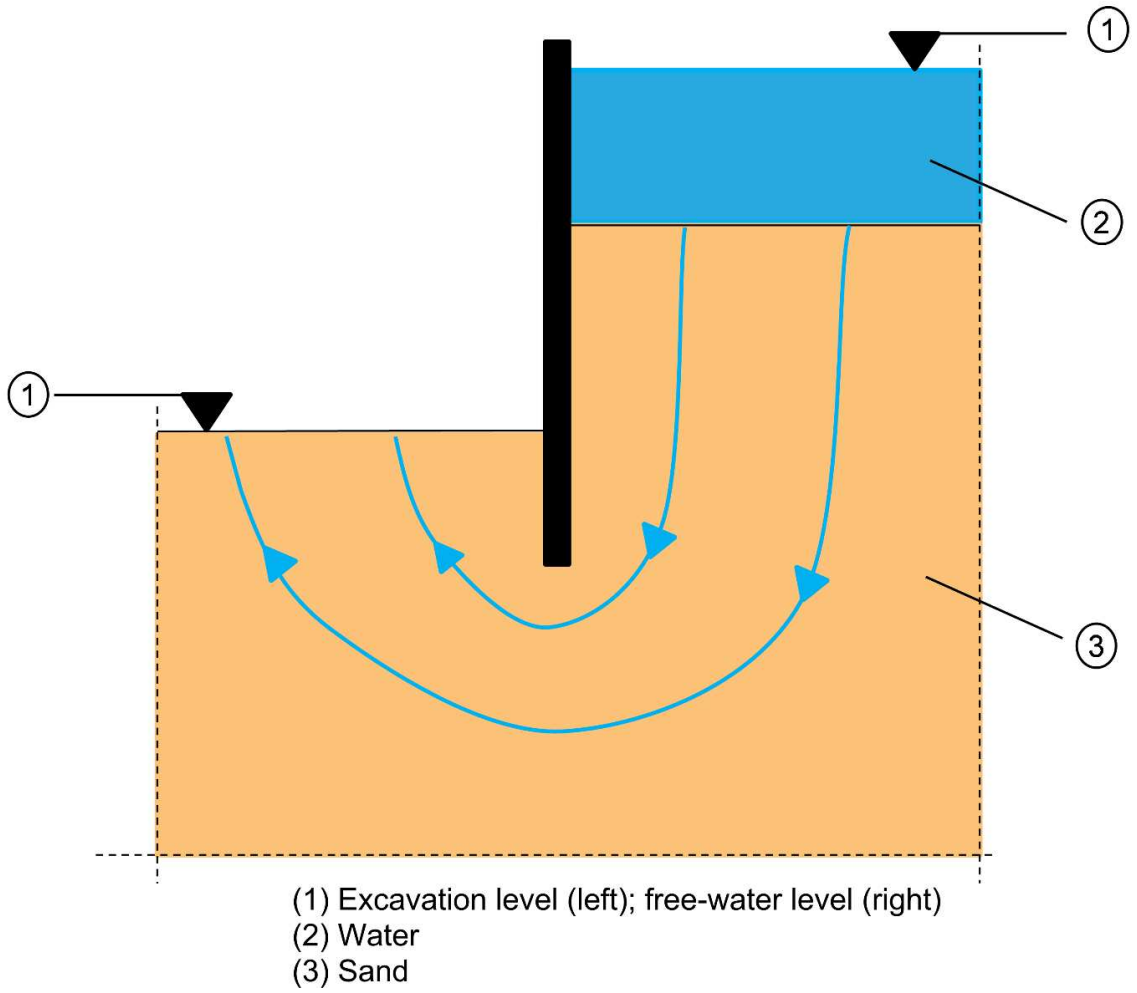

Figure 1. Example of situation where heave might be critical

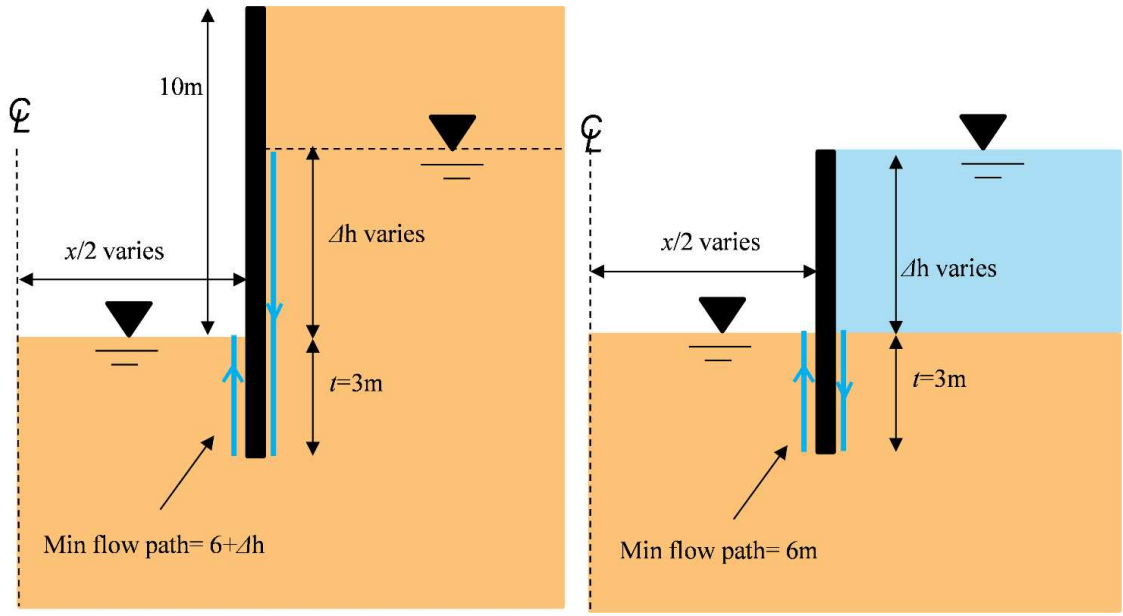

Figure 2. Geometry of the 10m excavation and the cofferdam reference models

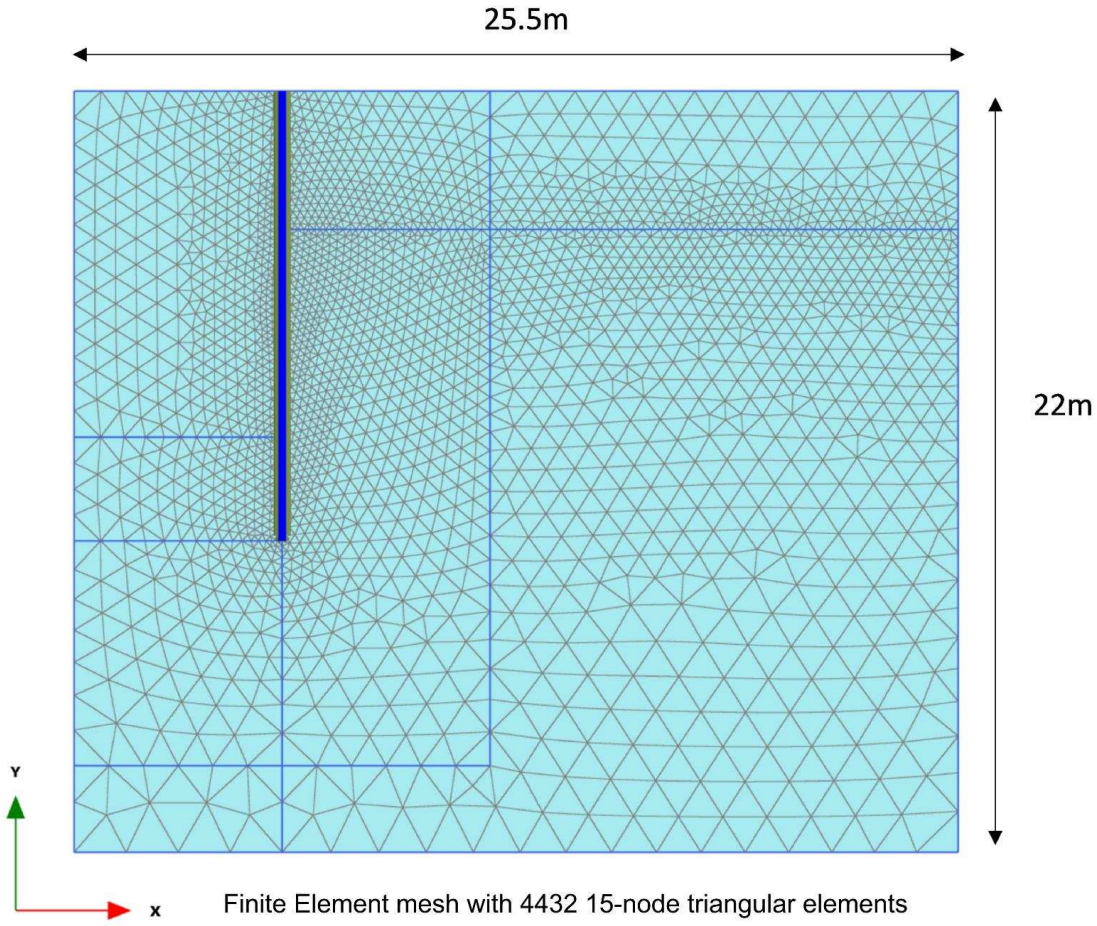

Figure 3. Finite Element mesh for the 10m deep excavation model

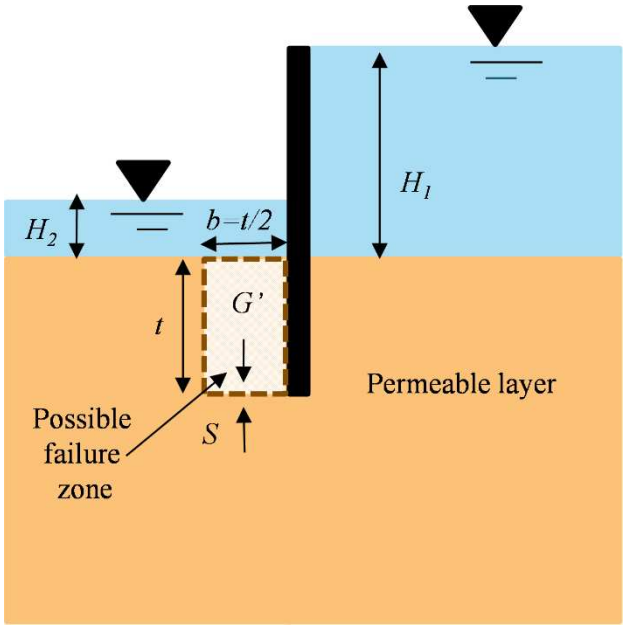

Figure 4. Terzaghi's calculation

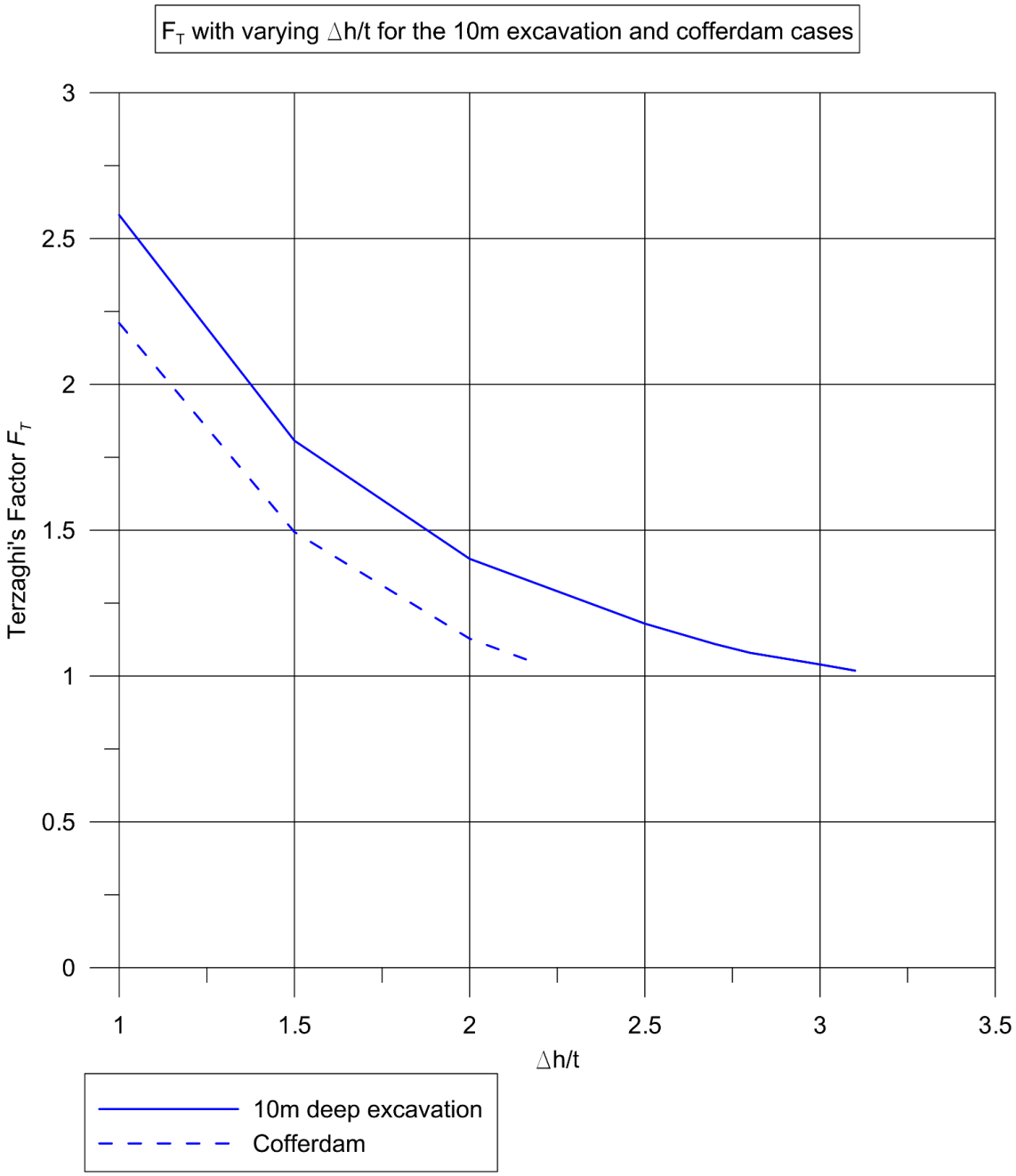

Figure 5. Calculated Terzaghi's factor with varying ⊿h/t for the 10m deep excavation and cofferdam cases

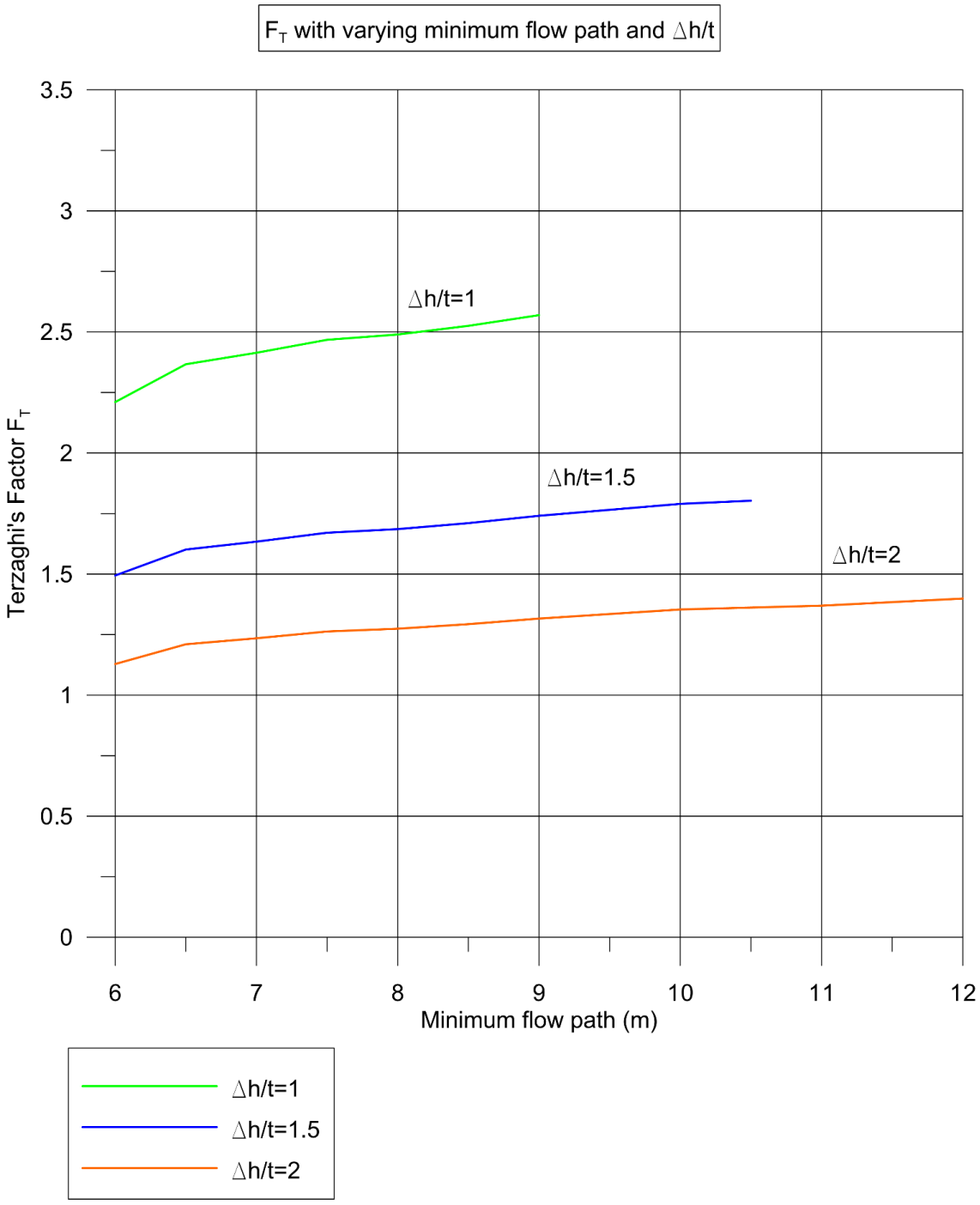

Figure 6. Calculated Terzaghi's factor with varying minimum flow path

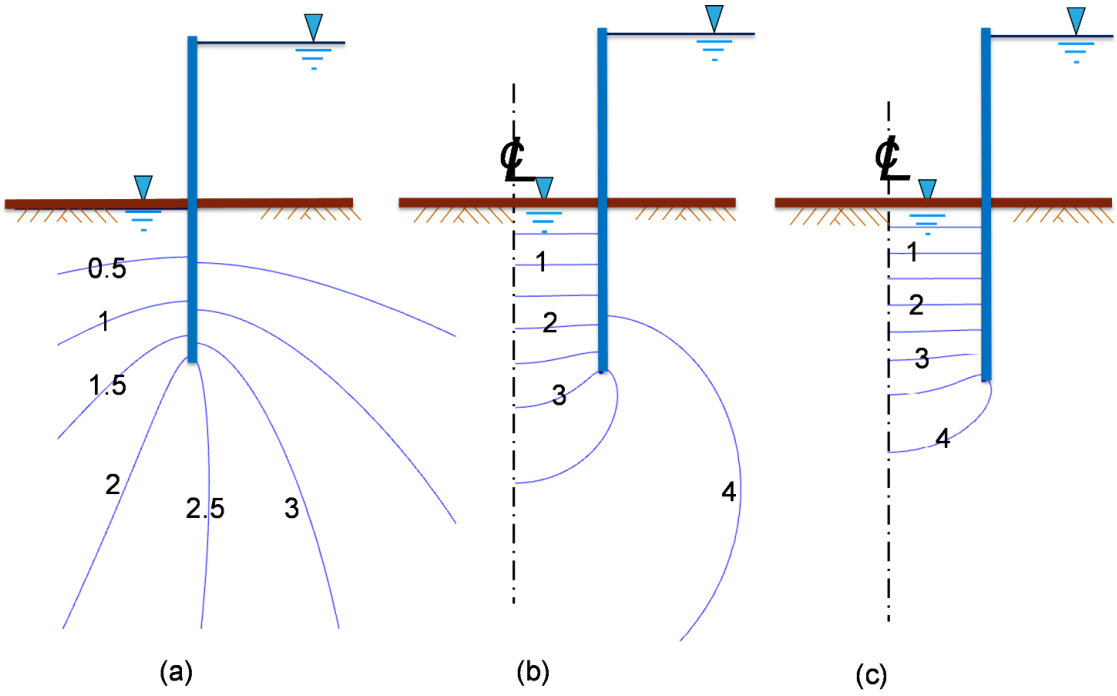

Figure 7. Equipotentials for three cases: (a) a wide excavation (width x=12t), (b) a narrow trench (x=t), and (c) a circular excavation (diameter d=t)

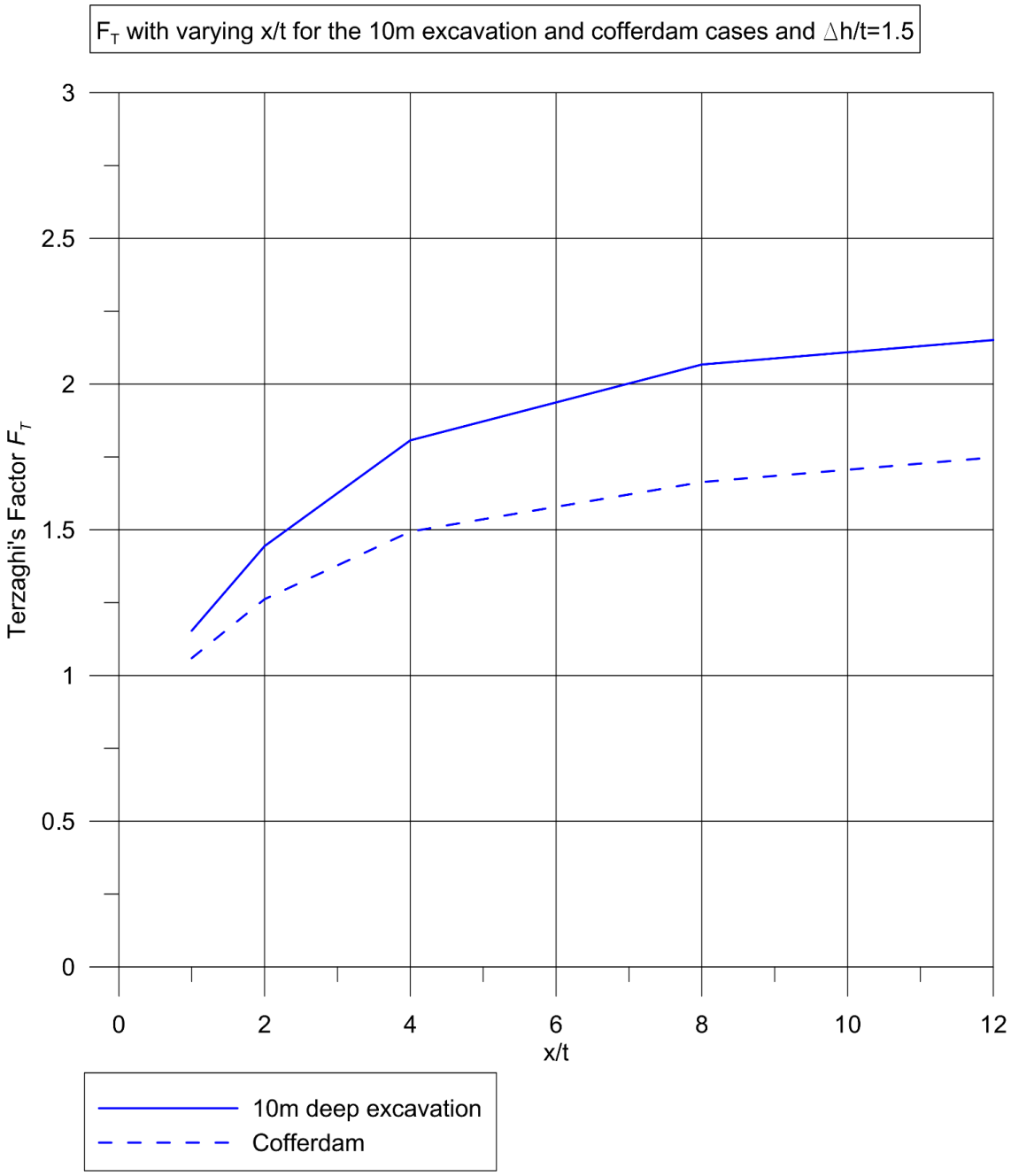

Figure 8. Calculated Terzaghi's factor with varying x/t for the 10m deep excavation and cofferdam cases with Δh/t=1.5

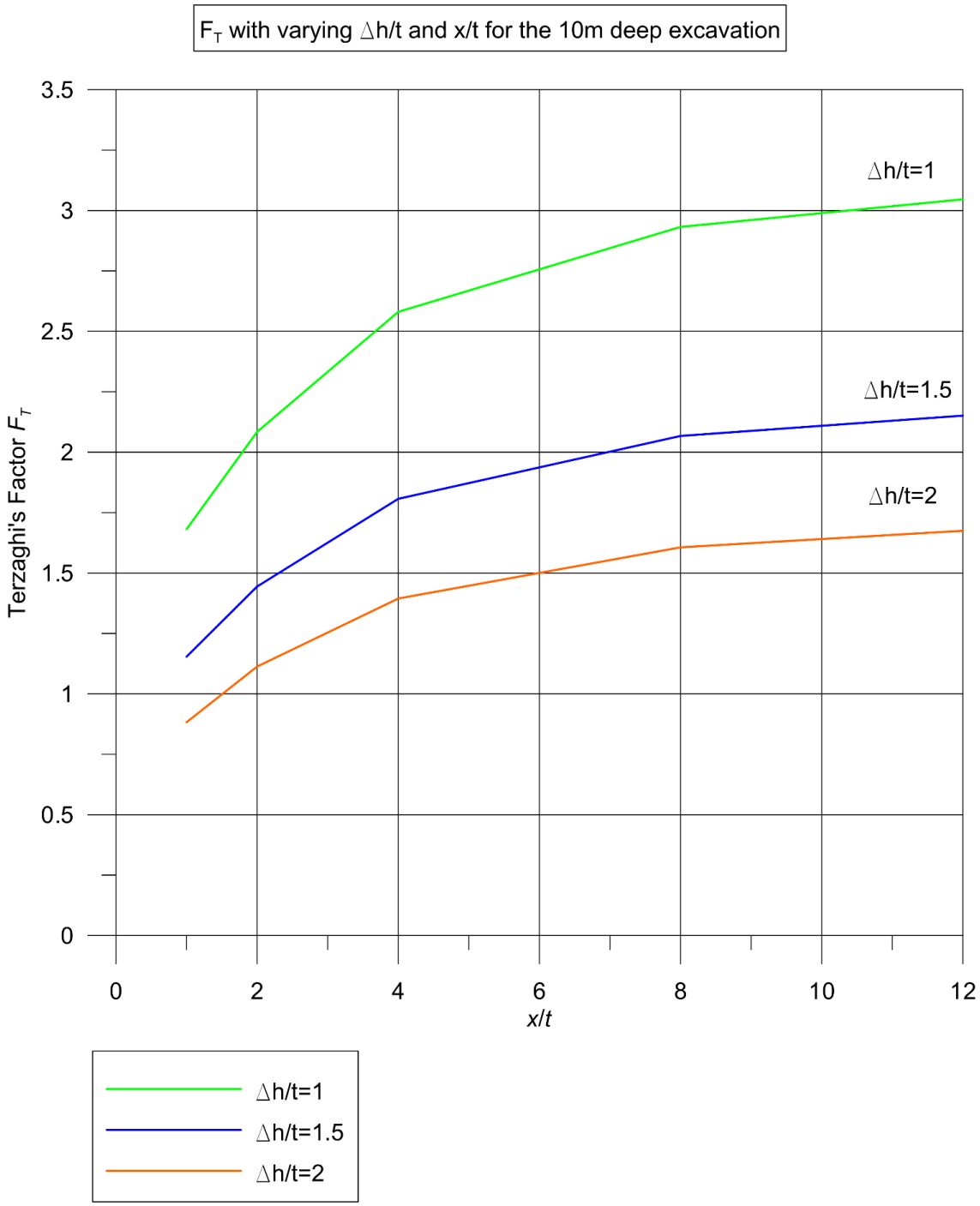

Figure 9. Calculated Terzaghi's factor for varying x/t and Δh/t for the 10m deep excavation problem

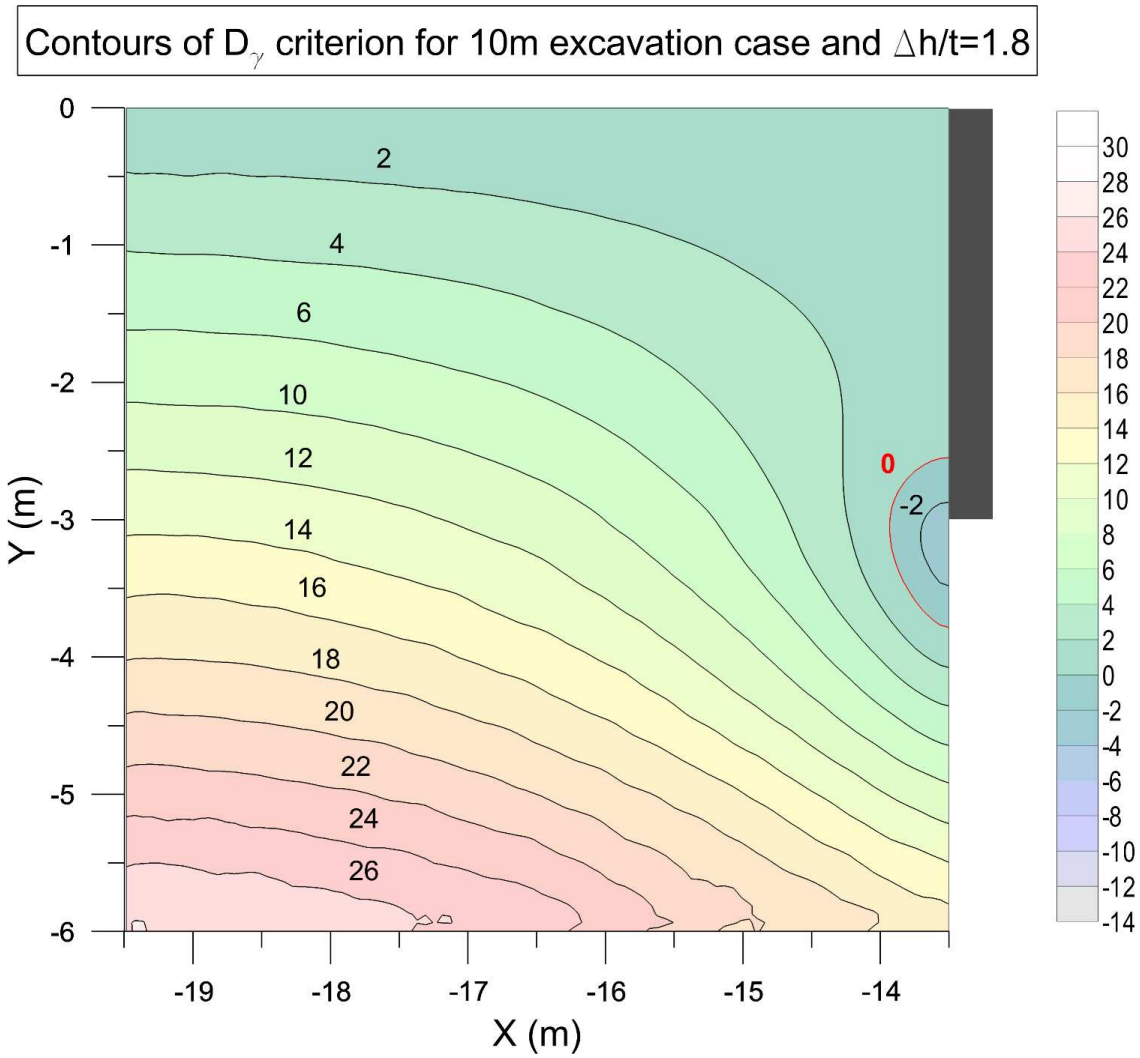

Figure 10. Contours of D_γ for the 10m excavation case with $\Delta h = 1.8t$

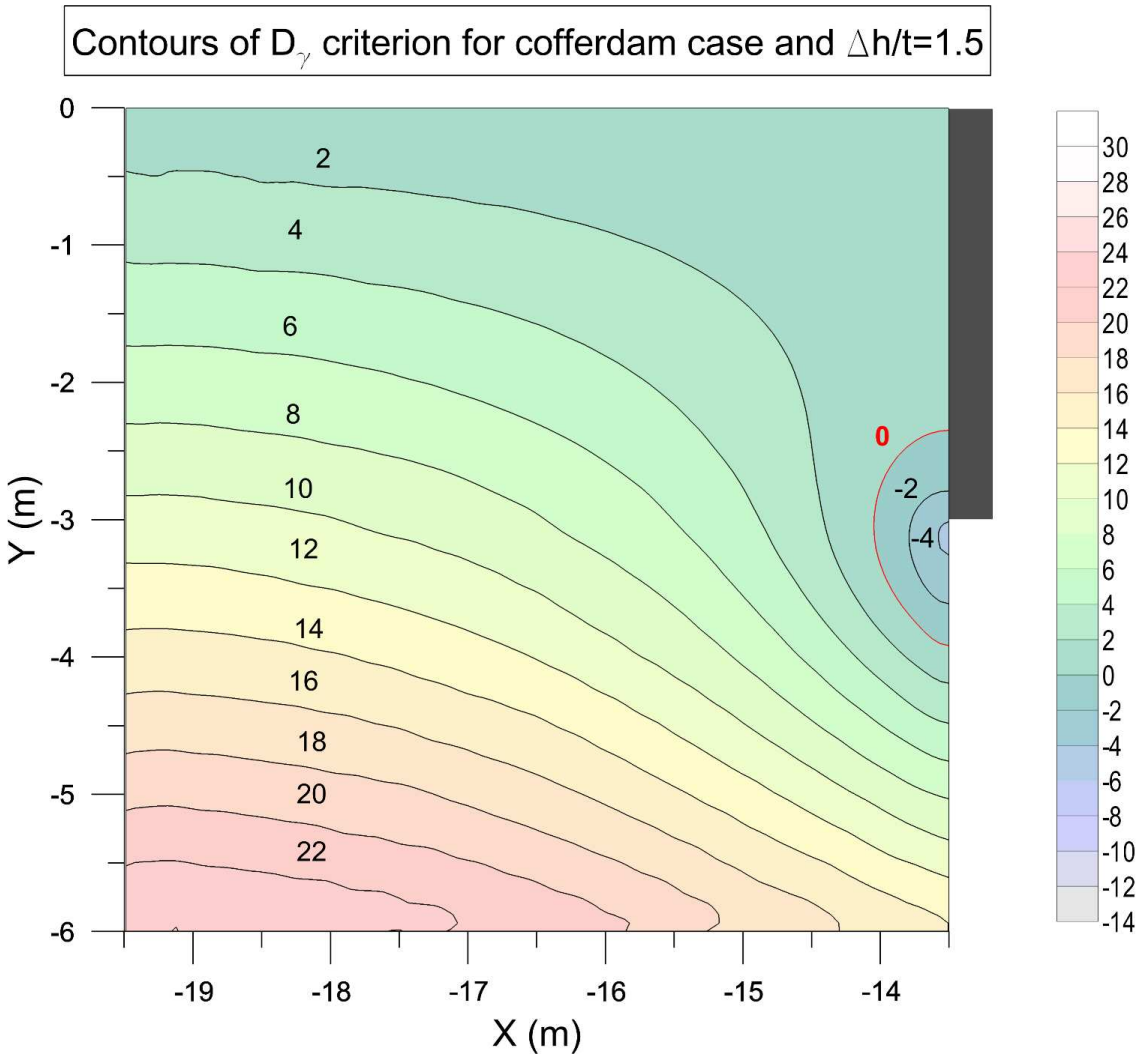

Figure 11. Contours of D_γ for the cofferdam case with $\Delta h = 1.5t$

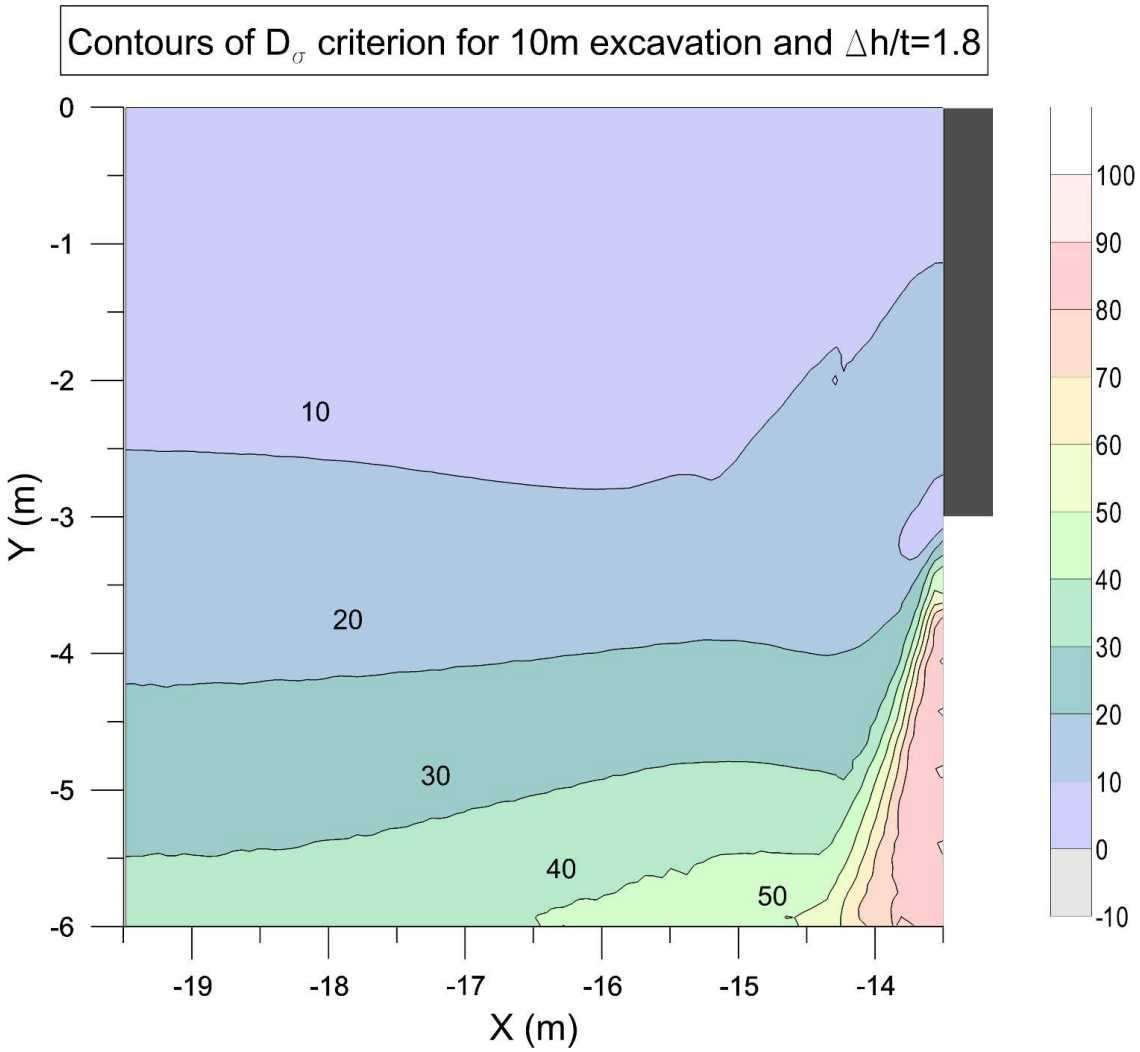

Figure 12. Contours of D_σ for the 10m excavation case with Δh = 1.8t

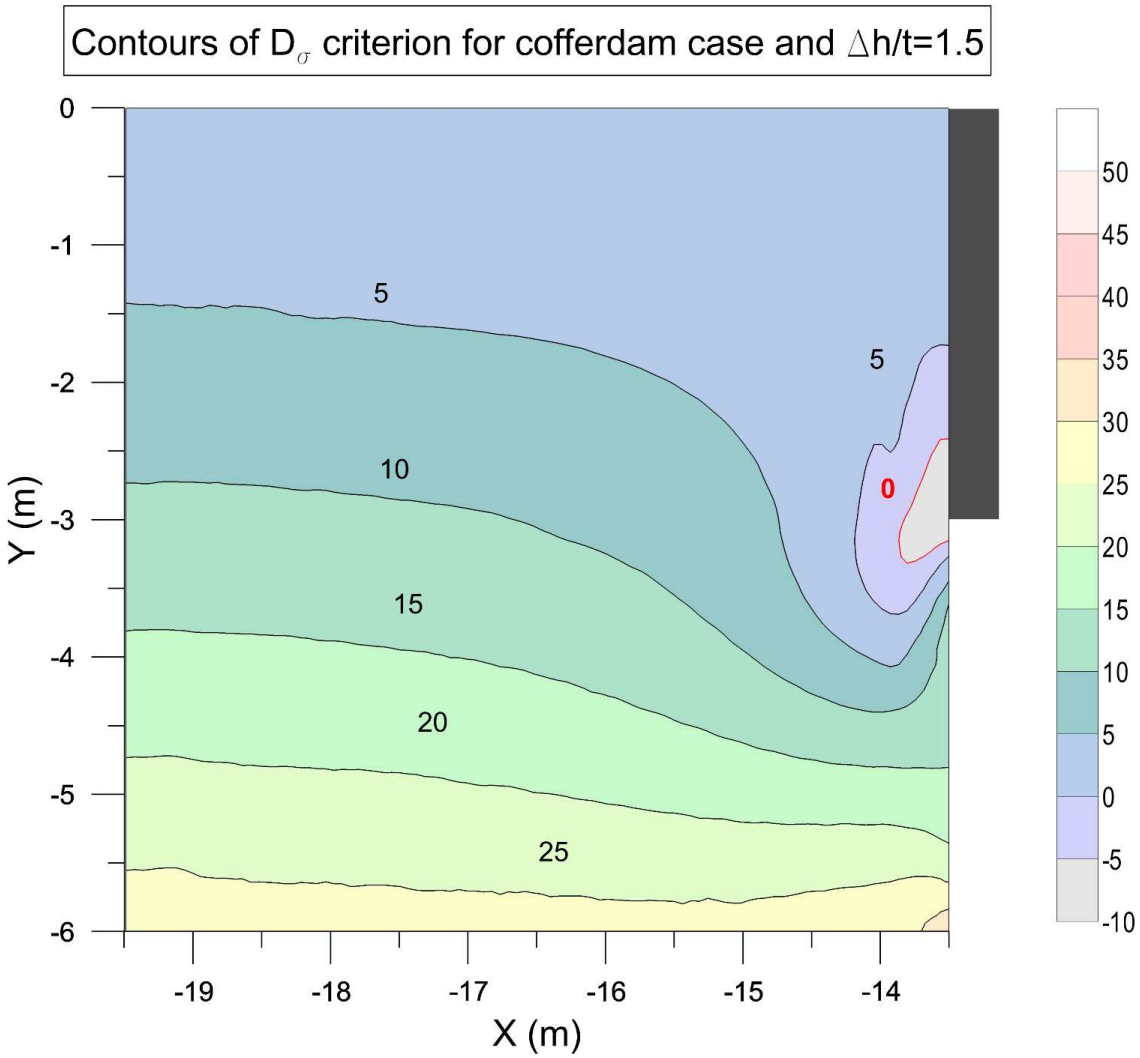

Figure 13. Contours of $\boldsymbol{D_\sigma}$ for the cofferdam case with Δh = 1.5t

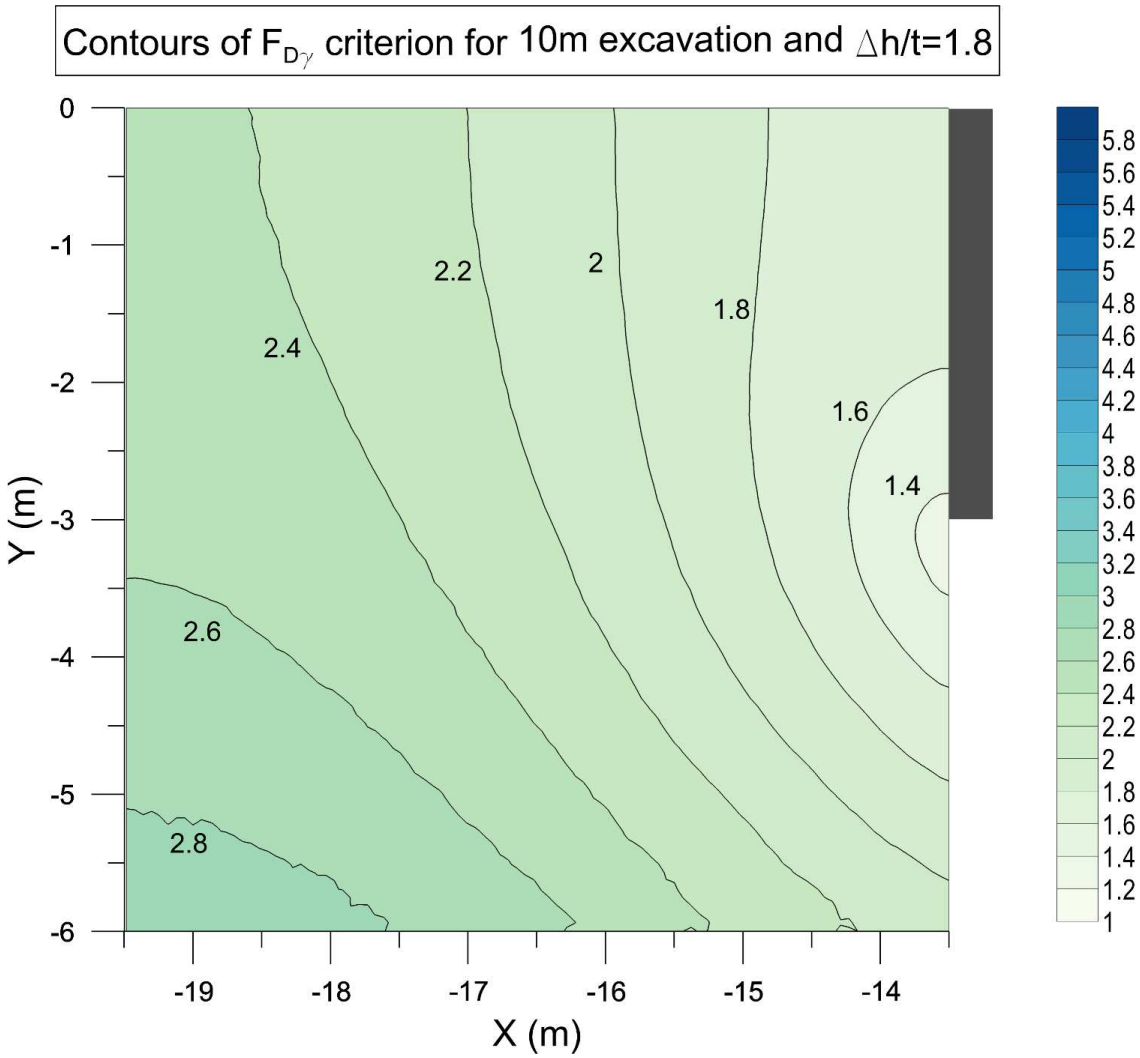

Figure 14. Contours of $F_{D\gamma}$ for the 10m excavation case with Δh = 1.8t

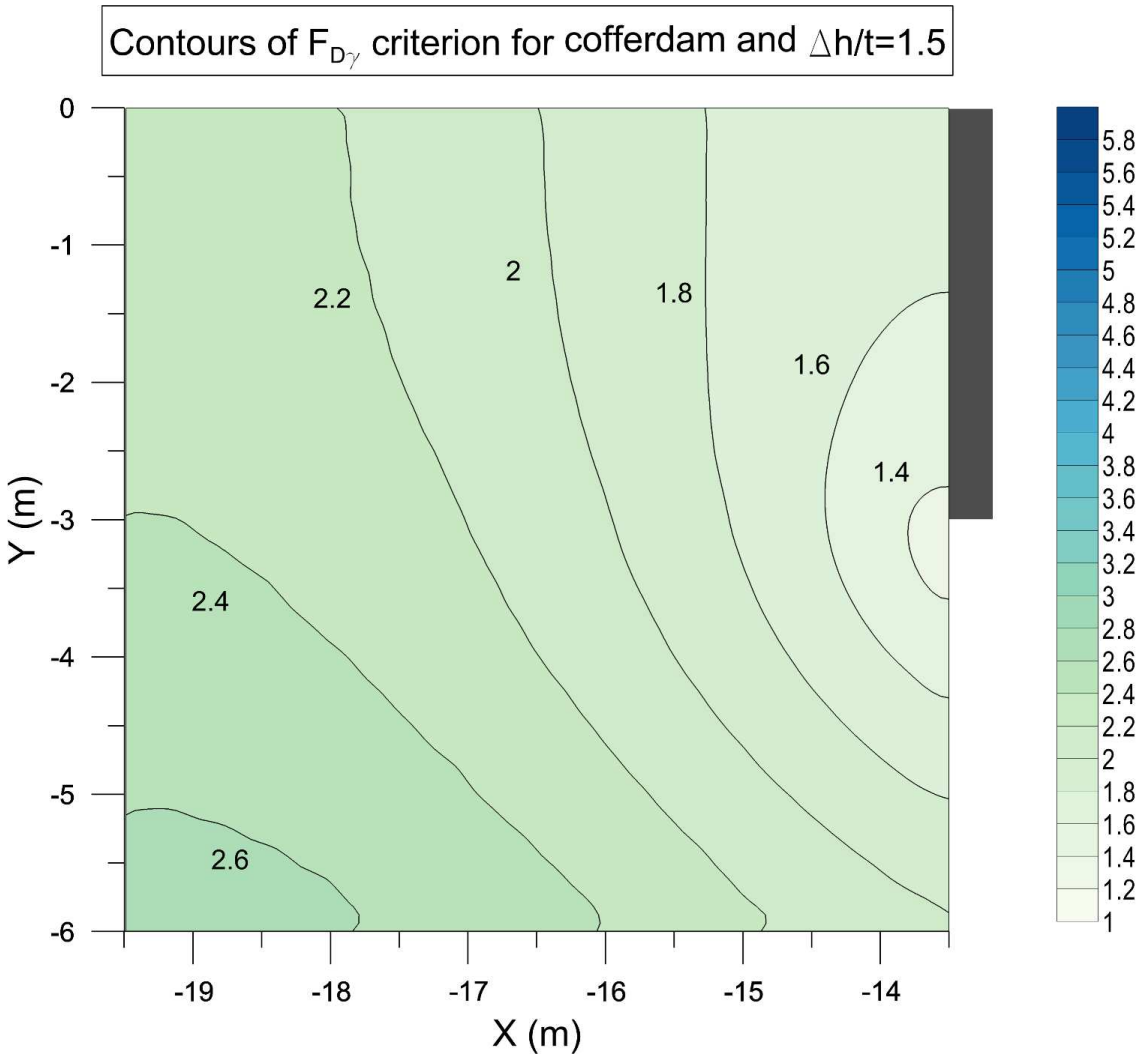

Figure 15. Contours of $F_{D\gamma}$ for the cofferdam case with Δh = 1.5t

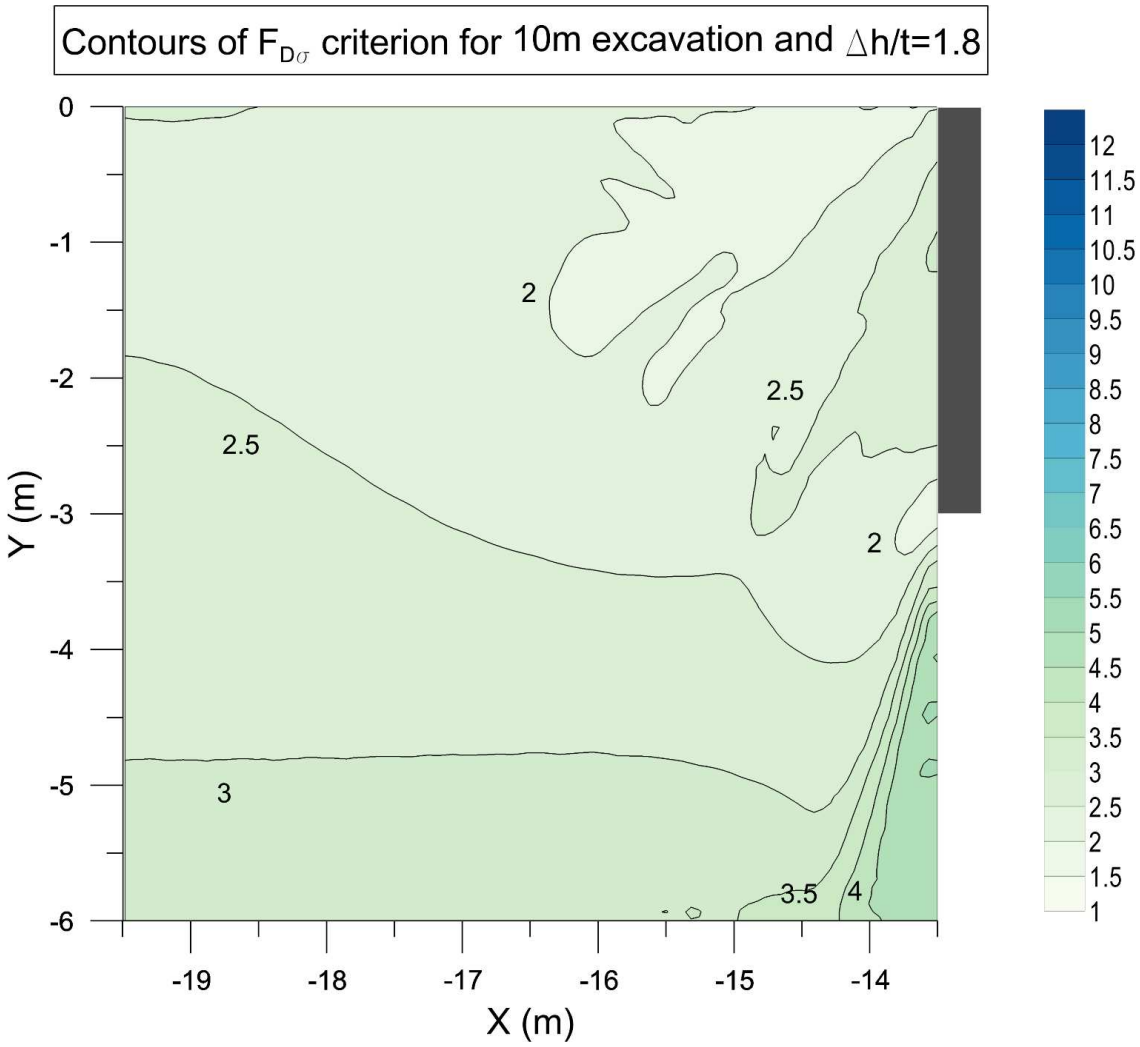

Figure 16. Contours of $F_{D\sigma}$ for the 10m excavation case with Δh = 1.8t

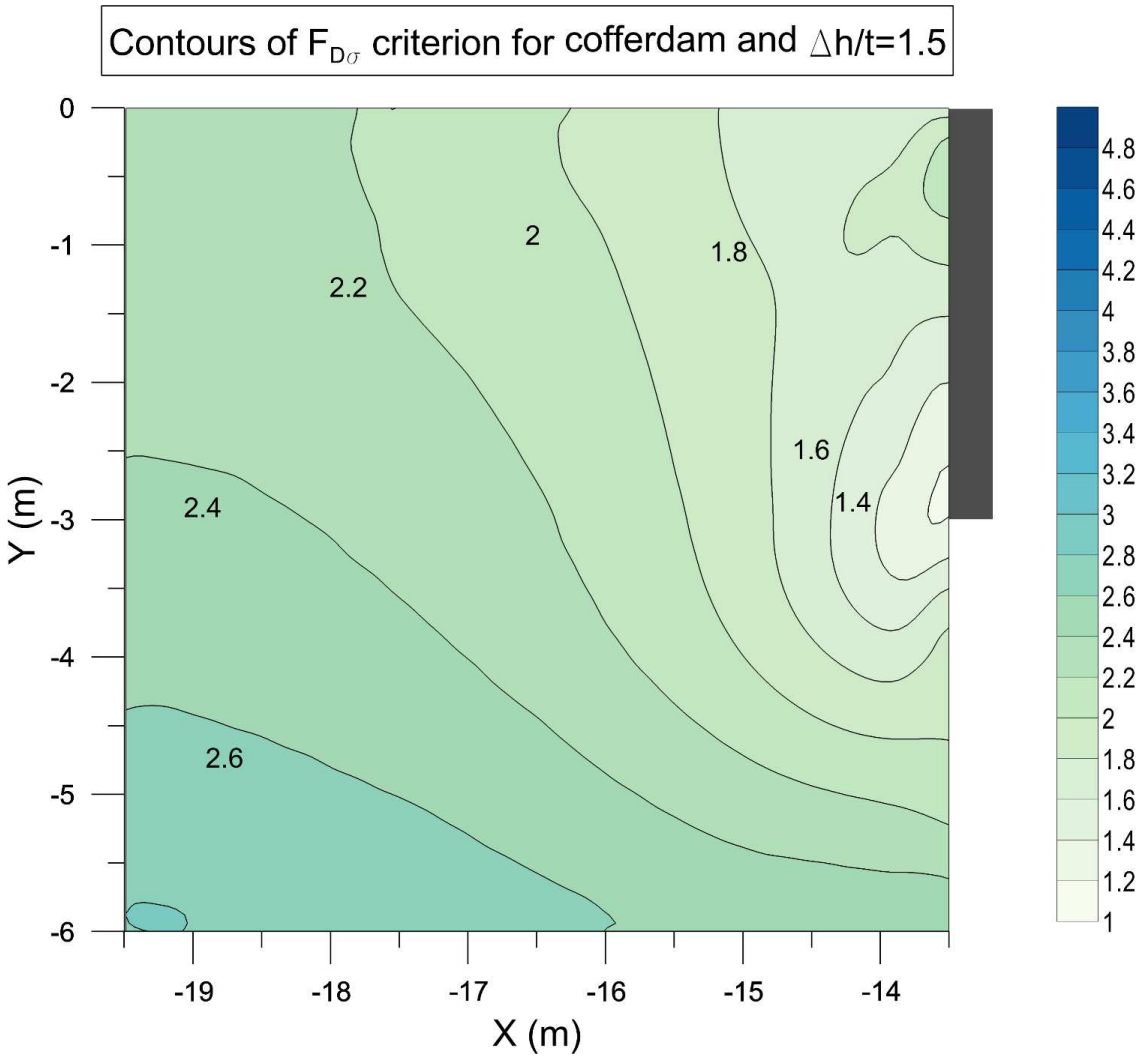

Figure 17. Contours of $F_{D\sigma}$ for the cofferdam case with Δh = 1.5t

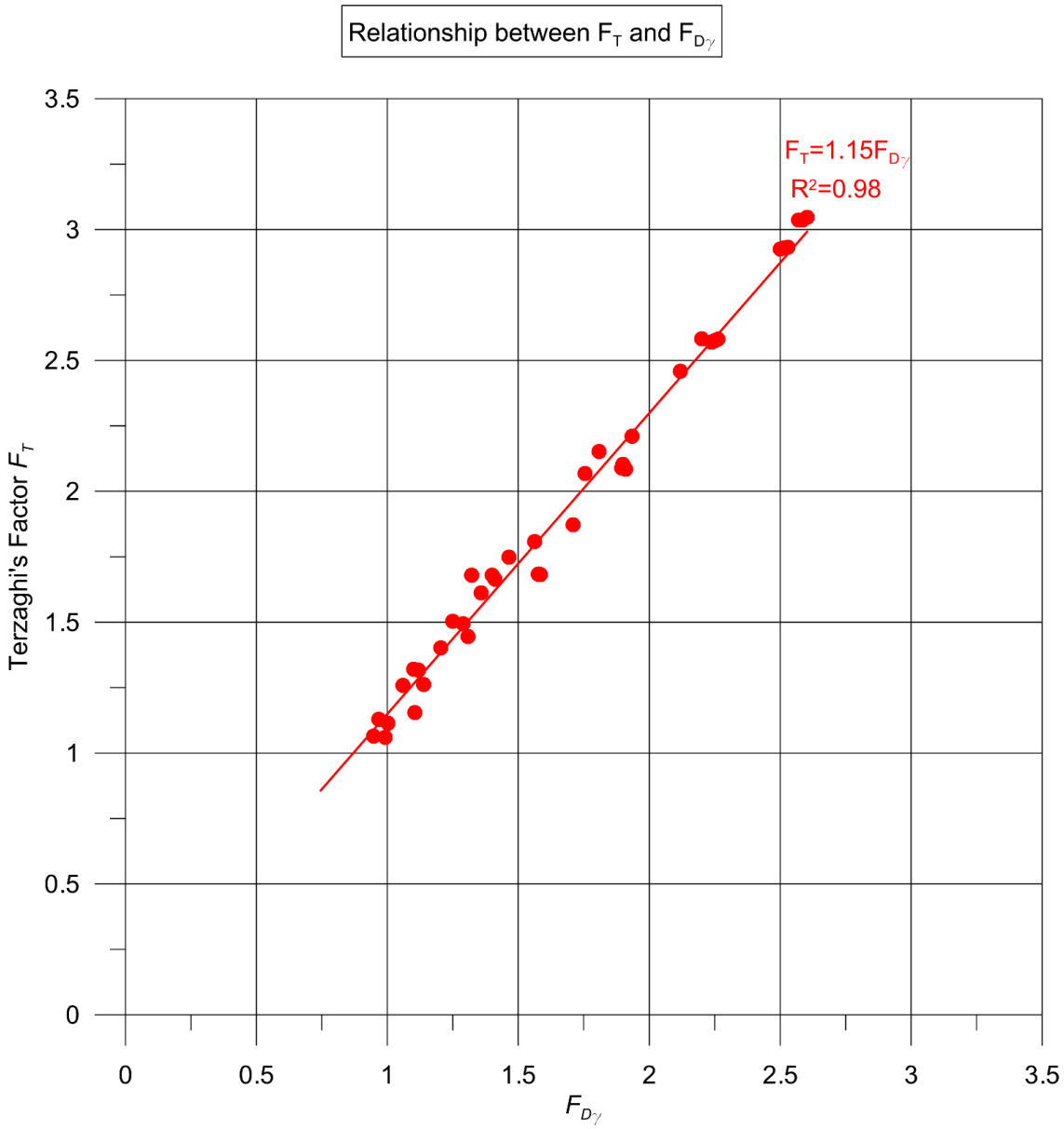

Figure 18. Relationship between the Terzaghi's factor F_T and the integration point approach factor $F_{D\gamma}$

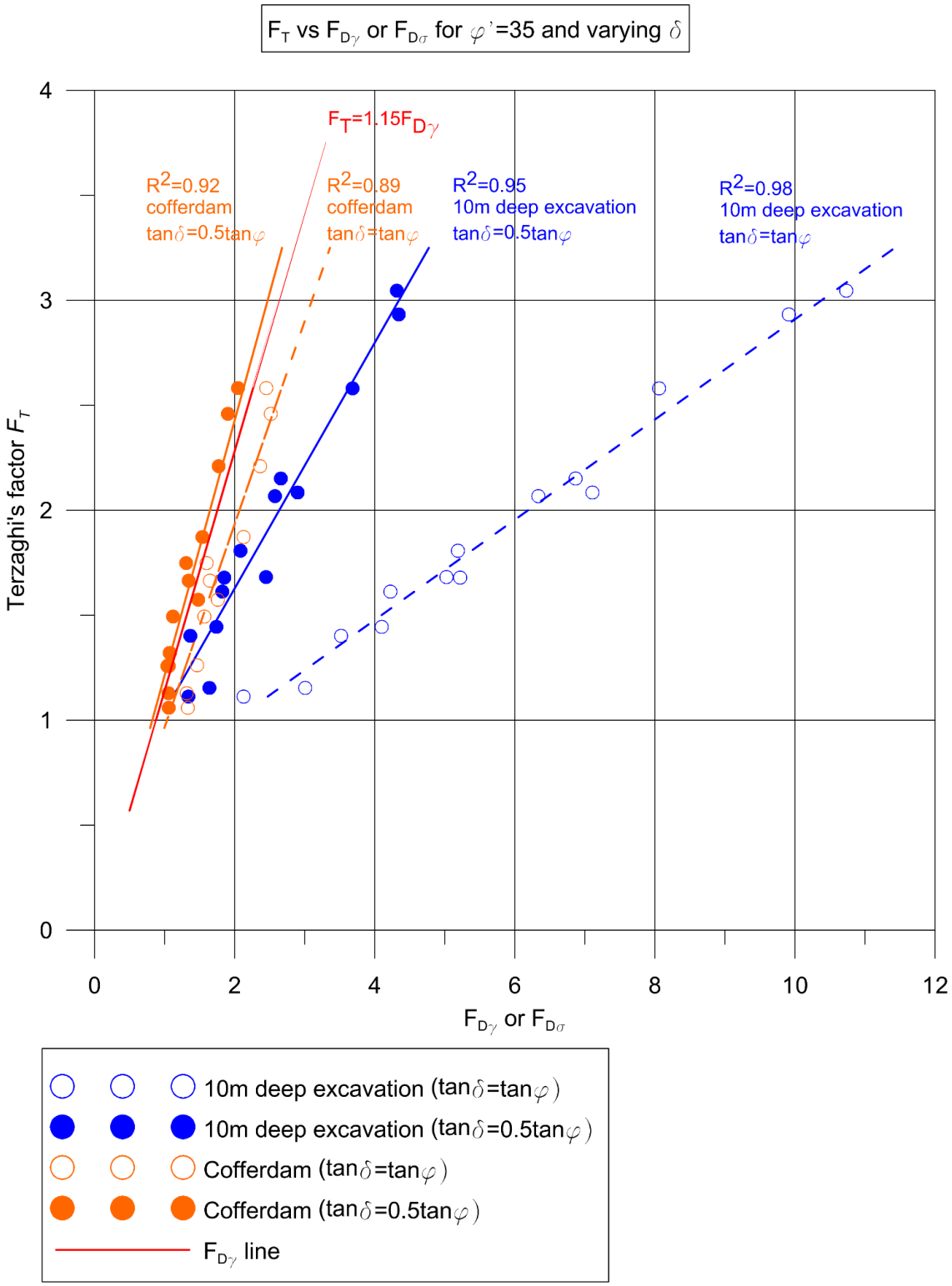

Figure 19. Relationship between the Terzaghi's factor F_T and the integration point approach factors $F_{D\gamma}$ and $F_{D\sigma}$ for φ'=35° and varying soil/wall friction angle δ.

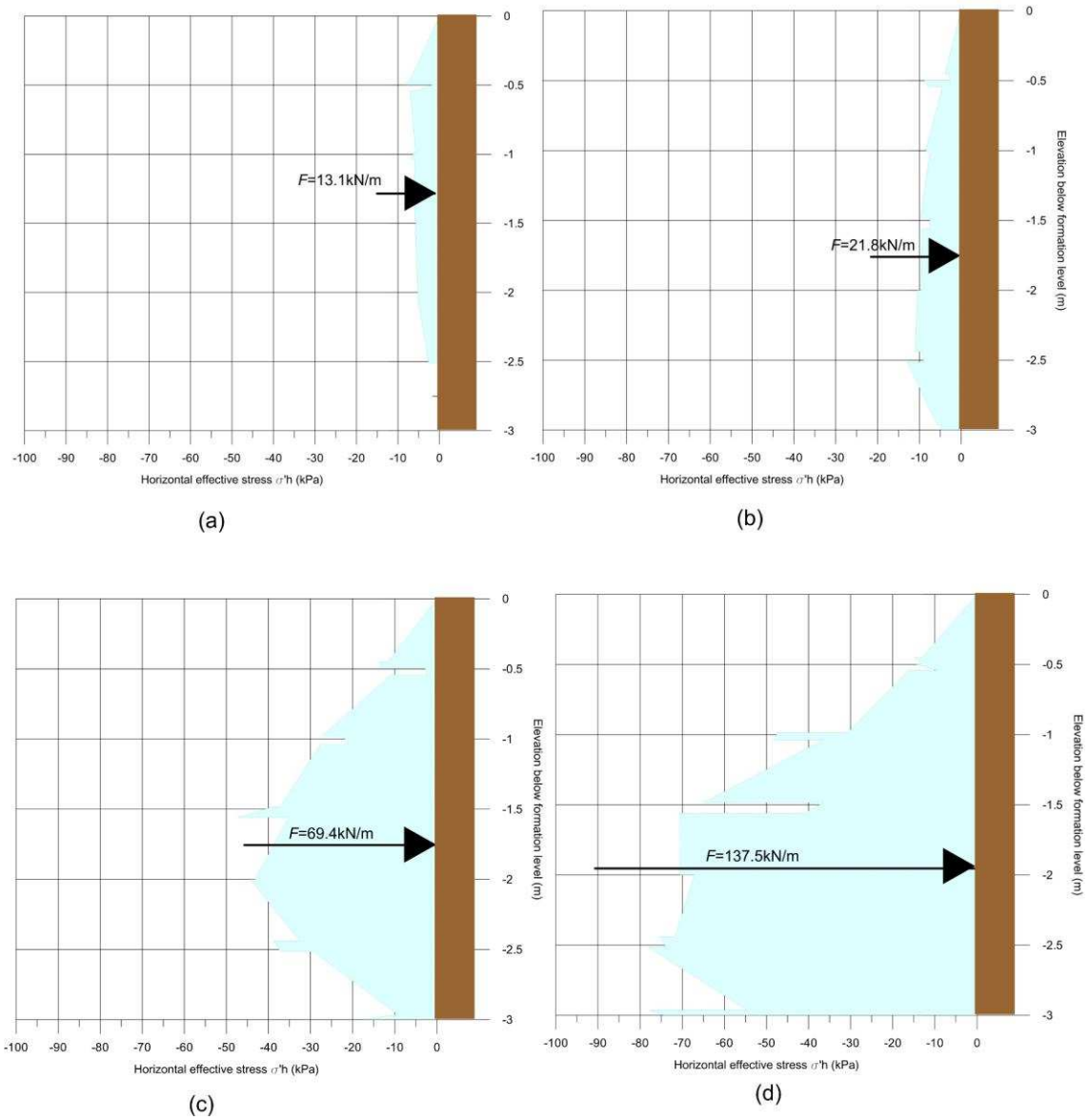

Figure 20. Horizontal effective stress distributions and resultant forces in front of the retaining wall for a) cofferdam with tanδ=0.5tanφ', b) cofferdam with $\delta=\varphi$', c) 10m deep excavation with tanδ=0.5tanφ' and d) 10m deep excavation with $\delta=\varphi$'.

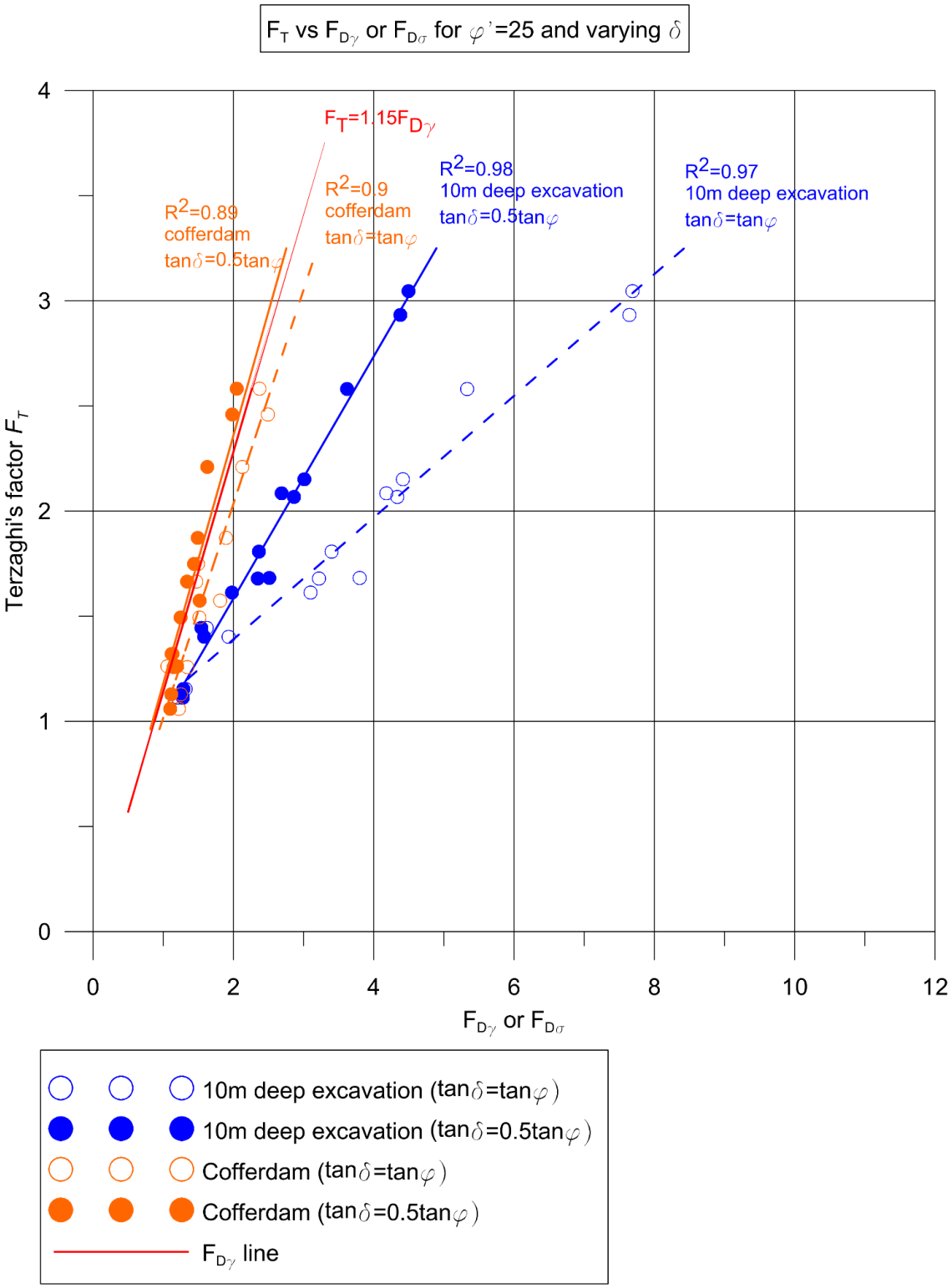

Figure 21. Relationship between the Terzaghi's factor F_T and the integration point approach factors $F_{D\gamma}$ and $F_{D\sigma}$ for φ'=25° and varying soil/wall friction angle δ.